

AD \_\_\_\_\_

Award Number: DAMD17-99-1-9120

TITLE: Comparative Structural Analysis of ERa and ERb Bound to  
Selective Estrogen Agonists and Antagonists

PRINCIPAL INVESTIGATOR: Geoffrey L. Greene, Ph.D.

CONTRACTING ORGANIZATION: The University of Chicago  
Chicago, Illinois 60637

REPORT DATE: July 2001

TYPE OF REPORT: Annual

PREPARED FOR: U.S. Army Medical Research and Materiel Command  
Fort Detrick, Maryland 21702-5012

DISTRIBUTION STATEMENT: Approved for Public Release;  
Distribution Unlimited

The views, opinions and/or findings contained in this report are  
those of the author(s) and should not be construed as an official  
Department of the Army position, policy or decision unless so  
designated by other documentation.

20011207 011

REPORT DOCUMENTATION PAGE			Form Approved OMB No. 074-0188	
Public reporting burden for this collection of information is estimated to average 1 hour per response, including the time for reviewing instructions, searching existing data sources, gathering and maintaining the data needed, and completing and reviewing this collection of information. Send comments regarding this burden estimate or any other aspect of this collection of information, including suggestions for reducing this burden to Washington Headquarters Services, Directorate for Information Operations and Reports, 1215 Jefferson Davis Highway, Suite 1204, Arlington, VA 22202-4302, and to the Office of Management and Budget, Paperwork Reduction Project (0704-0188), Washington, DC 20503				
1. AGENCY USE ONLY (Leave blank)		2. REPORT DATE July 2001		3. REPORT TYPE AND DATES COVERED Annual (14 Jun 00 - 13 Jun 01)
4. TITLE AND SUBTITLE Comparative Structural Analysis of ER $\alpha$ and ER $\beta$ Bound to Selective Estrogen Agonists and Antagonists			5. FUNDING NUMBERS DAMD17-99-1-9120	
6. AUTHOR(S) Geoffrey L. Greene, Ph.D.				
7. PERFORMING ORGANIZATION NAME(S) AND ADDRESS(ES)  The University of Chicago Chicago, Illinois 60637  E-Mail: gggreen@uchicago.edu			8. PERFORMING ORGANIZATION REPORT NUMBER	
9. SPONSORING / MONITORING AGENCY NAME(S) AND ADDRESS(ES)  U.S. Army Medical Research and Materiel Command Fort Detrick, Maryland 21702-5012			10. SPONSORING / MONITORING AGENCY REPORT NUMBER	
11. SUPPLEMENTARY NOTES Report contains color				
12a. DISTRIBUTION / AVAILABILITY STATEMENT Approved for Public Release; Distribution Unlimited				12b. DISTRIBUTION CODE
13. ABSTRACT (Maximum 200 Words) The goal of this investigation is to determine the three-dimensional structures of the two known human estrogen receptors (ER $\alpha$ and ER $\beta$ ) complexed with receptor-selective estrogens and antiestrogens (SERMs). The crystallographic structures of ER $\alpha$ and ER $\beta$ ligand binding domains complexed with <i>cis</i> -R,R-diethyl-tetrahydrochrysene-2,8-diol (R,R-THC) have been solved and refined, suggesting mechanisms by which this compound can act as an ER $\alpha$ agonist and as an ER $\beta$ antagonist. Agonists and antagonists bind at the same site within the core of the ER LBD to induce distinct conformations in the transactivation domain (AF-2), especially in the positioning of helix 12. Previously determined structures of ER $\alpha$ with 4-hydroxytamoxifen (OHT) and diethylstilbestrol (DES) revealed and defined a multipurpose docking site on ER $\alpha$ and ER $\beta$ that can accommodate either helix 12, in the presence of OHT, or one of several co-regulators in the presence of DES. R,R-THC stabilizes a conformation of the ER $\alpha$ LBD that favors coactivator association and a conformation of the ER $\beta$ LBD that prevents coactivator association. A comparison of the two structures, combined with functional data, reveals that THC does not act on ER $\beta$ through the same mechanisms used by other known ER antagonists. Instead, THC antagonizes ER $\beta$ through a novel mechanism we term "passive antagonism". Paradoxically, the R,R-THC-ER $\beta$ structure is very similar to the structure induced by genistein, which acts as a partial estrogen through both ER subtypes. Ongoing mutagenesis studies should help define the molecular and structural differences that are responsible for these unanticipated results. The passive antagonism mechanism suggests a novel approach to the design of ligands that selectively antagonize the two ER subtypes. Such ligands may have novel therapeutic properties that can be exploited to prevent or treat breast cancer.				
14. SUBJECT TERMS Estrogen receptors alpha and beta (ER $\alpha$ and ER $\beta$ ); receptor structure; x-ray crystallography; selective estrogen receptor modulators (SERMs); agonism versus antagonism; passive antagonism				15. NUMBER OF PAGES 58
				16. PRICE CODE
17. SECURITY CLASSIFICATION OF REPORT Unclassified	18. SECURITY CLASSIFICATION OF THIS PAGE Unclassified	19. SECURITY CLASSIFICATION OF ABSTRACT Unclassified	20. LIMITATION OF ABSTRACT Unlimited	

# ANNUAL REPORT FOR Award Number DAMD17-99-1-9120

## TABLE OF CONTENTS

	Page Numbers
Front Cover.....	1
SF 298 Report Document .....	2
Table of Contents .....	3
Introduction.....	4
Body.....	4-13
Task 1 .....	4
Task 2 .....	5-9
Task 3 .....	9-13
Key research accomplishments.....	13
Reportable outcomes.....	13-14
Conclusions.....	14-15
References .....	15-16
Appendix .....	17

## INTRODUCTION

The goal of this investigation is to determine the three-dimensional structures of the two known human estrogen receptors (ER $\alpha$  and ER $\beta$ ) complexed with receptor-selective estrogens and antiestrogens (SERMs). An important, unresolved issue is the molecular mechanism(s) by which SERMs can act selectively as full agonists, partial agonists, or complete antagonists in the control of cell proliferation and cell fate in different tissues. The physiological effects of both endogenous and synthetic SERMs are mediated by the estrogen receptors (ERs), ER $\alpha$  and ER $\beta$ , members of the nuclear receptor (NR) super-family of ligand-regulated transcription factors. The two ER subtypes have overlapping but distinct tissue distribution patterns *in vivo* and distinct activation profiles at both classical and complex promoter elements. Thus, it is unclear how ER $\alpha$  and ER $\beta$  individually contribute to the effects of known estrogens. Ligands that act differentially on ER $\alpha$  and ER $\beta$  would be potentially valuable both as tools to dissect the biological roles of the two ERs and as novel therapeutics with pharmacological properties distinct from existing drugs. As part of a search for ER subtype-selective ligands, the synthetic compound, R,R-5,11-*cis*-diethyl-5,6,11,12-tetrahydrochrysene-2,8-diol (R,R-THC), was identified as a selective estrogen agonist when bound to ER $\alpha$  and as an antagonist when bound to ER $\beta$ . To better understand this selective behavior, a major goal of this investigation was to determine the crystallographic structures of human ER $\alpha$  and ER $\beta$  ligand binding domains (LBDs) complexed with R,R-THC. These structures have now been solved and refined, suggesting mechanisms by which this compound can act as an ER $\alpha$  agonist and as an ER $\beta$  antagonist. Previously determined structures of ER $\alpha$  with 4-hydroxytamoxifen (OHT) and diethylstilbestrol (DES) (1) revealed and defined a multipurpose docking site on ER $\alpha$  and ER $\beta$  that can accommodate either helix 12, in the presence of OHT, or one of several co-regulators in the presence of DES. Thus, agonists and antagonists bind at the same site within the core of the ER LBD to induce distinct conformations in the transactivation domain (AF-2), especially in the positioning of helix 12. Interestingly, R,R-THC stabilizes a conformation of the ER $\alpha$  LBD that favors coactivator association and a conformation of the ER $\beta$  LBD that prevents coactivator association. A comparison of the two structures, combined with functional data, reveals that R,R-THC does not act on ER $\beta$  through the same mechanisms used by other known ER antagonists. Instead, R,R-THC antagonizes ER $\beta$  through a novel mechanism we term "passive antagonism". Paradoxically, the R,R-THC-ER $\beta$  structure is very similar to the structure induced by genistein (2), which acts as a partial estrogen through both ER subtypes. Ongoing mutagenesis studies should help define the molecular and structural differences that are responsible for these unanticipated results. In addition, the passive antagonism mechanism suggests a novel approach to the design of ligands that selectively antagonize the two ER subtypes. Such ligands may have novel therapeutic properties that can be exploited to prevent or treat breast cancer.

## BODY

The Statement of Work for this grant listed four major tasks. These tasks are listed below with details of the progress made toward achieving each goal.

### **Task 1 (First year): To produce and purify bacterially expressed ER $\alpha$ -LBD-BJK-1 complexes for biochemical analysis and crystallization.**

As described in detail in the attached manuscript (see Appendix) and in last year's Annual Report, this task has been accomplished. BJK-1 is the same as R,R-THC. We did not know the identity of BJK-1 at the time the proposal was submitted to the USAMRMC in 1998.

**Task 2 (Second year): Purification, crystallization, and x-ray analysis of ER $\alpha$ / $\beta$ -LBD-BJK-1 and ER $\alpha$ / $\beta$ -LBD-ICI complexes.**

The major portion of this task has been accomplished, as described in the attached manuscript (see Appendix) and in last year's Annual Report. We did not pursue either the ER $\alpha$ -or ER $\beta$ -ICI 182,780 complexes because the R,R-THC studies consumed all available personnel time for this grant. During this period, we learned that the Hubbard lab had solved the structure of rat ER $\beta$  LBD complexed with ICI 164,384; the structure was published earlier this year (3). Because this structure is expected to be identical to the human ER $\beta$  LBD complexed with ICI 182,780 and very similar to the ER $\alpha$  LBD complex, we abandoned this aim, although it may still be of some value to know if the ER $\alpha$ -ICI conformation is different from the ER $\beta$ -ICI conformation. Noteworthy in the ICI-ER $\beta$  structure was the absence of any association of the transactivation helix (H12) with the LBD, which contrasts with all other known antagonist-ER structures, in which H12 is associated with the hydrophobic cleft formed by helices 3, 4 and 5 (**Appendix, Figure 2A**). In the ICI-ER $\beta$  complex, the terminal portion of the ICI bulky side chain substituent emerges from the ligand-binding pocket and binds to part of the coactivator recruitment site (AF2), thereby preventing H12 from adopting either its characteristic agonist or antagonist orientation (**Figure 1**). This complete destabilization of H12 may contribute to the more potent antiestrogenic activity of both closely related ICI compounds when compared to

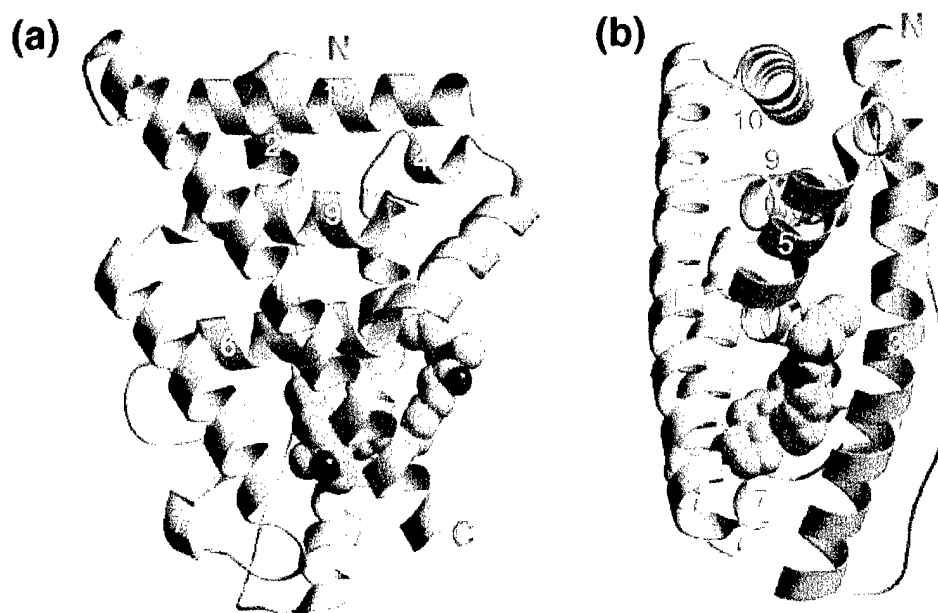


**Figure 1.** Structure (orthogonal views) of ER $\beta$ -LBD bound to the pure antagonist ICI 164,384. Reproduced from Pike et al. (3).

SERMs like tamoxifen and raloxifene. Another potentially significant difference is the effect of the ICI 164,384 on the ER $\beta$  dimerization interface. For all other known ER $\alpha$ / $\beta$  LBD structures, the ligand has little effect on the nature or extent of the dimer interface. However, ICI appears to generate a more open and perhaps less stable

dimer, consistent with reports that ER $\alpha$ -ICI dimers are less stable than other ligand-ER complexes (4). It is also possible that a crystallization artifact is responsible for the observed ICI-induced conformation, or that the ER $\beta$  dimer interface is more sensitive than ER $\alpha$  to ligand effects (3). For ER $\beta$ -R,R-THC, the dimer interface is very similar to the ER $\beta$ -Ral and ER $\beta$ -Gen structures (2, 3).

Analysis of protein structure is always a work in progress and the R,R-THC-ER $\alpha$ / $\beta$  LBD structures are no exception. Although we were able to obtain preliminary crystallographic solutions for both the R,R-THC-ER $\alpha$  and R,R-THC-ER $\beta$  LBD structures more than a year ago, ongoing data refinement during the past year revealed a more complex ligand interaction with the ER $\beta$  pocket than proposed initially. As shown in **Figure 2**, our original assumption that fewer contacts between R,R-THC and the amino acid residues that line the pocket of ER $\beta$  were responsible for the inability of this complex to assume an agonist conformation was incorrect. Instead, an equal or greater number of contacts occur between R,R-THC and amino acids that comprise the ligand-binding pocket, as compared to the R,R-THC-ER $\alpha$  LBD complex (**Appendix, Figure 4B**). The ER $\alpha$  complex structure has now been refined to a crystallographic R factor of 20.3% ( $R_{\text{free}} = 24.2\%$ ) using data to 1.95 Å resolution and the ER $\beta$  complex structure has been refined to a crystallographic R factor of 26.5% ( $R_{\text{free}} = 30.4\%$ ) using data to 2.85 Å resolution (**Appendix, Table 1**). It proved especially difficult to obtain an  $R_{\text{free}}$  value of 30.4% for ER $\beta$ , which is why we did not initially see the additional contacts that were present between R,R-THC and the ER $\beta$  LBD pocket. For example, we did not initially see the additional hydrogen bond that occurs between the A ring phenolic OH of R,R-THC and Arg 346, similar to the interaction with Arg 394 in the R,R-THC-ER $\alpha$  structure (**Figure 2B; Appendix, Figure 4B**). Similarly, additional R,R-THC contacts with the ER $\beta$  LBD pocket could only be appreciated

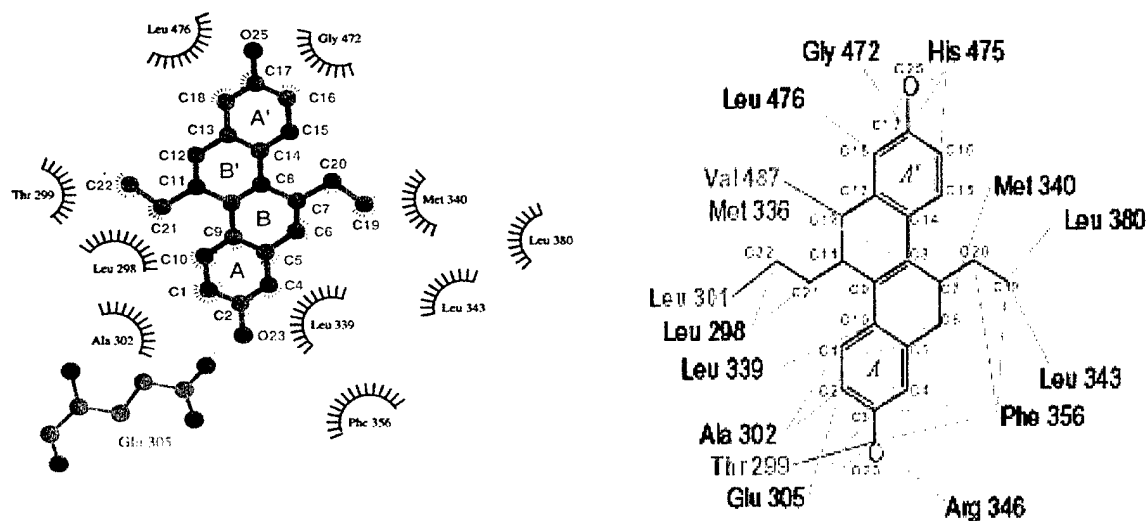


**Figure 2.** R,R-THC Interactions with ER $\beta$  LBD Pocket. **A.** Previous model. **B.** Current model based on refined structure (see **Appendix, Figure 4B**).

upon further refinement of the structural data. We now feel that there are some 16 amino acids, rather than the 11 first observed (**Figure 2B; Appendix, Figure 4B**), that participate in the stabilization of R,R-THC in ER $\beta$ , which equals the 16 amino acids that are involved in the R,R-THC-ER $\alpha$  LBD complex, although not all residues are the same (**Appendix, Figure 4B**).

Thus, although our hypothesis of “passive antagonism” has not changed, our view of the underlying mechanism(s) has evolved. As described previously, the ER $\beta$  LBD shares the same overall fold as the ER $\alpha$  LBD (**Appendix, Figure 2A**) (2). And like the ER $\alpha$  LBD, the ER $\beta$  LBD recognizes R,R-THC with a ligand-binding pocket located within its lower sub domain.

However, the binding of R,R-THC to the ER $\beta$  LBD does not stabilize the agonist-bound conformation of helix 12 (**Appendix, Figure 2A**). Neither is helix 12 bound to the portion of the coactivator recognition groove formed by helices 3, 4, and 5 as it is in the OHT-ER $\alpha$  LBD (1), RAL-ER $\alpha$  LBD (5), and RAL-ER $\beta$  LBD (2) complexes (**Appendix, Figure 2B**), nor is it disordered as it is in the ICI-ER $\beta$  LBD complex (**Figure 1**) (3). Instead, helix 12 in the R,R-THC-ER $\beta$  LBD complex interacts with the rest of the LBD in a manner most like that observed in the GEN-ER $\beta$  LBD complex (**Appendix, Figure 2B**) (2). Helix 12 is positioned similarly, and of comparable length (residues 487 to 498 in the R,R-THC complex and residues 487 to 497 in the GEN complex) in the two structures (**Appendix, Figure 2B**).

Based on previous correlations between the positioning of H12 and the ability of ER $\alpha$  and other NRs to form coactivator complexes, the conformation of the ER $\beta$  LBD observed in both the R,R-THC and GEN complexes should be incapable of interacting with coactivators and, hence, should be transcriptionally silent for two reasons. First, key residues from helix 12 (Leu 490, Glu 493, and Met 494) that are predicted to form part of the coactivator recognition surface are inappropriately positioned. In addition, helix 12 itself is bound such that it partially occludes the static region of the coactivator-binding surface formed by residues from helices 3, 4, and 5. Yet, GEN and R,R-THC clearly exhibit different activities on ER $\beta$  in mammalian cells; GEN acts as a partial agonist (6) and R,R-THC acts as a pure antagonist (7, 8). How can the similarity of the two structures be reconciled with the different activities of these compounds in transcriptional assays? The simplest model that explains these and other data is based on two suppositions (**Appendix, Figure 3A**). First, helix 12 in the unliganded ER $\beta$  LBD is in equilibrium between the R,R-THC/GEN-bound conformation, which precludes coactivator association, and the agonist-bound conformation seen in the E2- and DES-ER $\alpha$  LBD structures, which favors coactivator association (with the “inactive” R,R-THC/GEN-bound conformation being heavily favored). Second, rather than stabilizing a single static conformation of helix 12, ligands serve to shift the balance of this equilibrium. It is also highly likely that the coactivator receptor-interaction domain (e.g. GRIP NR box II domain) plays an active role in shifting this equilibrium.

R,R-THC could antagonize receptor activity by shifting equilibrium in favor of the inactive R,R-THC/GEN-bound conformation (**Appendix, Figure 3A**). If R,R-THC binding forces the receptor to favor this conformation even more than it does in the absence of ligand, the R,R-THC-receptor complex would be expected to have an even lower affinity for coactivator than the unliganded receptor. This would be consistent with the absence of transcriptional activity of the R,R-THC-ER $\beta$  complex and the conformation of helix 12 observed in the crystal.

Because the conformational equilibrium of helix 12 would be difficult to observe directly, we chose to test the hypothesis that the binding of different ligands should modulate the affinity of the ER $\beta$  LBD for coactivator such that E2-LBD  $\sim$  DES-LBD > GEN-LBD > apo-LBD > R,R-THC-LBD. The affinities of various ligand-ER $\beta$  LBD complexes for an LXXLL motif-containing peptide were therefore directly measured using a fluorescence polarization-based binding assay (**Appendix, Figure 3B**) (9). The full agonist complexes bind the peptide approximately 1.5-fold more tightly than the GEN complex ( $K_d$ [E2] = 0.36  $\mu$ M and  $K_d$ [DES] = 0.41  $\mu$ M versus  $K_d$ [GEN] = 0.58  $\mu$ M). In addition, the GEN complex binds the peptide more tightly than the unliganded receptor ( $K_d$ [apo] = 2.1  $\mu$ M), whereas the R,R-THC complex ( $K_d$ [R,R-THC] = 3.7  $\mu$ M) binds the peptide significantly weaker than the unliganded receptor.

Thus, these data are entirely consistent with the described helix 12 conformational equilibrium model. Furthermore, recent mutational and crystallographic data suggest that the positioning of helix 12 in ER $\alpha$  (10) and other NRs (11) is also dictated by a ligand-sensitive conformational equilibrium.

To better define and understand "passive antagonism", or antagonism without side chains, one has to consider the differences between classical estrogen antagonists, which contain bulky side chains, and molecules like R,R-THC. Although agonists and antagonists bind at the same site within the core of the LBD, each induces distinct conformations in the transactivation domain (AF-2) of the LBD, especially in the positioning of helix 12, providing structural evidence for multiple mechanisms of selective antagonism in the nuclear receptor family. Interestingly, the OHT/RAL and DES/E2 structures collectively reveal and define a multipurpose docking site on ER $\alpha$  that can accommodate either helix 12 or one of several coregulators. In addition, a comparison of the two types of structures reveals that there are at least two distinct mechanisms by which structural features of OHT promote an inhibitory conformation of helix 12 (1, 5). Helix 12 positioning is determined both by steric considerations, such as the presence of an extended side chain in the ligand, and by local structural distortions in and around the ligand binding pocket. Thus, one would predict that effective estrogen antagonists do not necessarily require bulky or extended side chains.

The positioning of the side chains of OHT, RAL, and ICI directly or "actively" preclude the agonist-bound conformation of helix 12 by steric hindrance. Hence, we define their common mechanism of action as "active antagonism". Clearly, R,R-THC does not have a bulky side chain (**Appendix, Figure 1A**), and in its complex with ER $\beta$ , helix 12 is not sterically precluded from adopting the agonist-bound conformation as it is in the other antagonist complexes (**Appendix, Figures 2A and 4C**). Instead, R,R-THC antagonizes ER $\beta$  by stabilizing key ligand binding pocket residues in noninteracting conformations, and disfavoring the equilibrium to the agonist-bound conformation of helix 12. Thus, we term the mechanism of antagonism of R,R-THC as "passive antagonism". Passive antagonism may not be unique to R,R-THC and ER $\beta$ . There are many examples of NR ligands, which act as antagonists even though they are smaller than the endogenous agonists of these NRs. The synthetic androgen receptor antagonist, flutamide, is comparable in size to testosterone, and does not possess an obvious moiety that would act as an antagonist side chain (12).

Many NRs have multiple subtypes, that possess distinct expression patterns and that regulate distinct target genes. Antagonists generated through the addition of bulky side chains to agonist scaffolds are limited to being antagonistic on one or more subtypes of a particular NR. The passive antagonism mechanism, as revealed here through direct comparison of the two R,R-THC-ER LBD complexes, suggests a new approach to achieving NR antagonism. Compounds could be designed to selectively stabilize the inactive conformations of certain NR subtypes and the active conformations of others. Such ligands may exert novel biological and therapeutic effects.

A manuscript describing the above data was recently submitted to *Nature Structural Biology* for review (included in the Appendix). Clearly, significant progress was made during the past year



in our effort to understand the unique R,R-THC-induced conformation of ER $\beta$  that contributes to "passive antagonism". More on this subject is included in the summary of Tasks 3 & 4 below.

**Tasks 3 & 4 (Third year): To compare and correlate structural differences among hER $\alpha/\beta$ -LBD complexes with the biological activity of hER $\alpha/\beta$ .**

Work on these tasks has already begun and we have made significant progress in trying to understand the contributions of residues that line the ligand-binding pocket to ligand discrimination between ER $\alpha$  and ER $\beta$ . An effort to crystallize ER $\alpha$  and/or ER $\beta$  complexed with GW5638 is also under way in the lab, but the main effort related to this grant during the coming year will be to better understand what distinguishes ER $\alpha$  from ER $\beta$  in their ability to differentially recognize diverse ligands with unique behavior. We will also begin modeling ligands that should have predictable agonist or antagonist properties as we learn more about the similarities and differences between the two ER subtypes from our own structures and those reported by others in the field. In addition, we will continue to create and test the ability of mutant ERs to interact with known coactivators and/or corepressors and to act as selective transcription modulators in co-transfection assays.

As described above, R,R-THC does not behave as an ER $\beta$  agonist. Instead, it binds to ER $\beta$  without interacting with several residues that it contacts in ER $\alpha$ , and by forming alternative hydrogen bonds and additional packing contacts not observed in the ER $\alpha$  complex (**Appendix, Figures 4B and 4C**). Hence, R,R-THC is able to bind to the ER $\beta$  LBD without nucleating many of the equivalent cooperative interactions observed in the ER $\alpha$  complex. For example, in the ER $\alpha$  complex the side chain of Met 528 packs against the side chains of His 524 and Met 343, stabilizing the helical conformation of the flanking residues. Because R,R-THC binding favors alternative conformations of His 475 and Met 295 (equivalent to His 524 and Met 343, respectively), the side chain of Met 479 (equivalent to Met 528) is completely disordered in the ER $\beta$  complex. In fact, by stabilizing conformations of binding pocket residues that prevent their interaction, R,R-THC binding should actually disfavor the equilibrium to the agonist-bound conformation of helix 12 (**Appendix, Figures 3A and 3B**).

A key unanswered question relates to the molecular/structural differences between the two ER subtypes that allow R,R-THC to stabilize these distinct arrangements of ligand binding pocket residues. There are only two binding pocket residues which are not identical in the two subtypes: Leu 384 (from helix 5/6) and Met 421 (from helix 8) in ER $\alpha$ , which are equivalent to Met 336 and Ile 373, respectively, in ER $\beta$  (**Figure 3**) (13, 14). These two residue pairs are similarly positioned on opposite faces of R,R-THC in their respective complexes. In the ER $\alpha$  complex, Leu 384 and Met 421 form several nonpolar contacts with R,R-THC (**Appendix, Figures 4B and 4C**). By contrast, only Met 336 interacts with R,R-THC in the ER $\beta$  complex (**Appendix, Figures 4B and 4C**).

Modeling studies suggest that Met 336 and Ile 373 would adopt both different positions and different conformations (relative to their positions in the R,R-THC-ER $\beta$  complex) in the agonist-bound conformation of the ER $\beta$  LBD (**Appendix, Figure 5**). There is currently no published structure of ER $\beta$  bound to a full agonist. However, given its similarity to the E2-ER $\alpha$  and DES-ER $\alpha$  LBD complexes (outside of helix 12 and the loop connecting helices 11 and 12), the GEN-

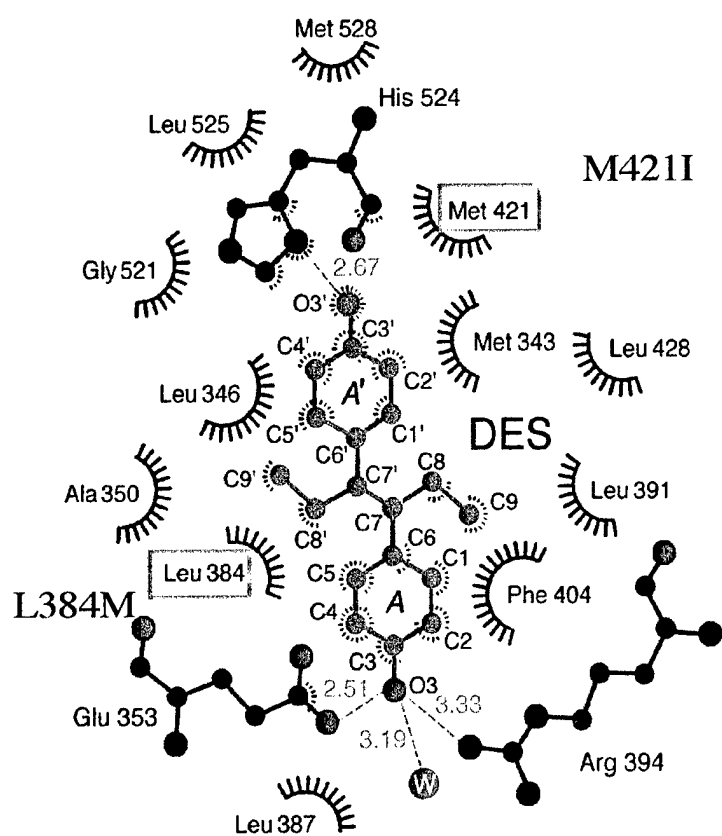


**Figure 3.** Comparison of amino acids that line the ligand-binding pocket of ER $\alpha$  LBD and ER $\beta$  LBD.

ER $\beta$  LBD complex (2) may serve as the basis for a model of the agonist-bound conformation of the ER $\beta$  LBD. In order for the A' ring region of R,R-THC to fit between the side chains of Met 336 and Ile 373 (in this model), R,R-THC would need to be positioned lower in the ER $\beta$  binding pocket relative to its location in the ER $\alpha$  binding pocket. This is because the side chain of Met 336 is larger than that of Leu 384, and conversely the side chain of Ile 373 is smaller than that of Met 421. This lower position should be highly unfavorable because it would result in a steric clash between both atoms of one of the R,R-THC ethyl groups with the side chain of Leu 298 at the floor of the pocket (**Appendix, Figure 5**). To avoid this unfavorable interaction, R,R-THC binds in the alternative mode observed in the crystal. Consistent with this hypothesis, the dimethyl analog of R,R-THC, which should be less

sterically hindered from adopting the lower position, acts as a weak ER $\beta$  partial agonist (7).

Because the conformational effects of ligand binding are cooperative in nature, residues that lie outside the binding pocket may also play roles the subtype-selective effects of R,R-THC. Nevertheless, preliminary mutagenesis results indicate that Leu 384/Met 336 and Met 421/Ile 373 do contribute to these effects (**Figure 4**), at least for ER $\alpha$ . However, the effect is only partial for ER $\alpha$  and the corresponding ER $\beta$   $\rightarrow$  ER $\alpha$  amino acid swapping mutations (Met336  $\rightarrow$  Leu384, Ile373  $\rightarrow$  Met421) do not result in the recovery of any detectable R,R-THC agonist activity (**Figure 4B**). The same result was observed both for full length ER $\alpha$  and ER $\beta$  (data not shown) as well as for the LBD of each ER fused to the Gal4 DNA binding domain. In both cases, a transcriptional activation assay was used to assess ER or ER LBD activity in transiently transfected MDA-MB-231 breast cancer cells in which recombinant GRIP1 was also co-expressed (see attached manuscript for experimental details). Estradiol and OHT were tested as positive and negative controls, respectively for both ER subtypes and behaved as expected with both single and double mutations (**Figure 4A**). In total, these results indicate that the two non-conserved amino acids that line the inside of the LBD pocket (**Figure 3**) are not sufficient for selective  $\alpha$  or  $\beta$  behavior in terms of response to R,R-THC. However, for other ligands, such as HPTE (**Figure 5**), these two amino acids do appear to play a major role in distinguishing between ER $\alpha$  and ER $\beta$  behavior (**Figure 4B**). While HPTE, an estrogenic metabolite of the

organochlorine pesticide methoxychlor, is a potent ER $\alpha$  agonist in HepG2 cells (15), it has minimal agonist activity with either human or rat ER $\beta$  and almost completely abolishes estradiol-induced ER $\beta$  activity. Notably, exchange of the two ER $\alpha$ / $\beta$ -distinguishing amino acids effectively converted ER $\alpha$  into ER $\beta$  and vice versa in a cell based reporter assay of HPTE activity (**Figure 4B, HPTE**). In contrast, the behavior of certain pyrazole derivatives, like

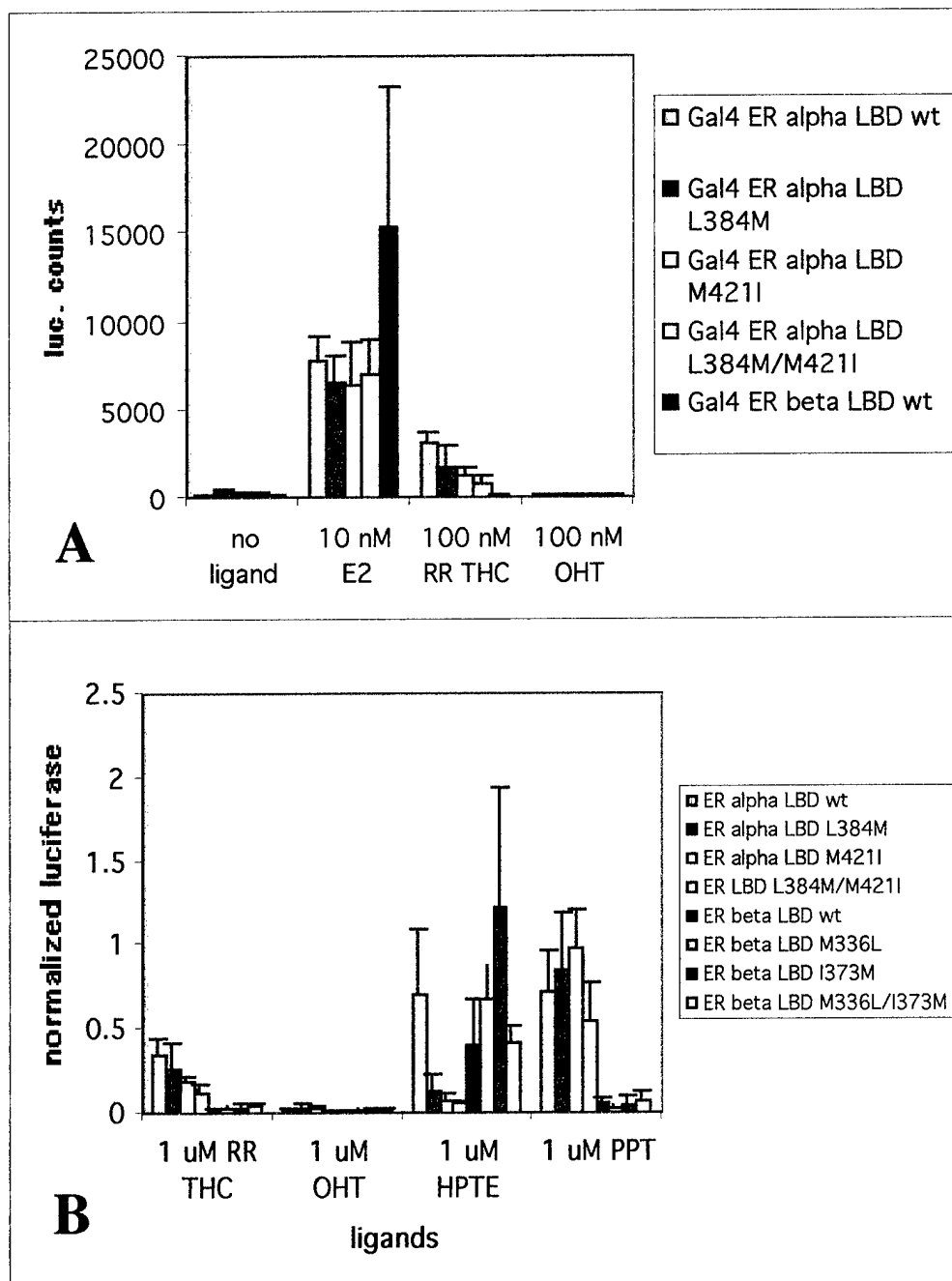


**Figure 4.** Transcriptional activity of Gal4-ER $\alpha$ / $\beta$  LBD mutants versus wild type ER $\alpha$ / $\beta$  LBDs (+ GRIP1; in MDA-MB231 cells). **A.** Positive and negative controls. **B.** ER subtype-selective ligands.

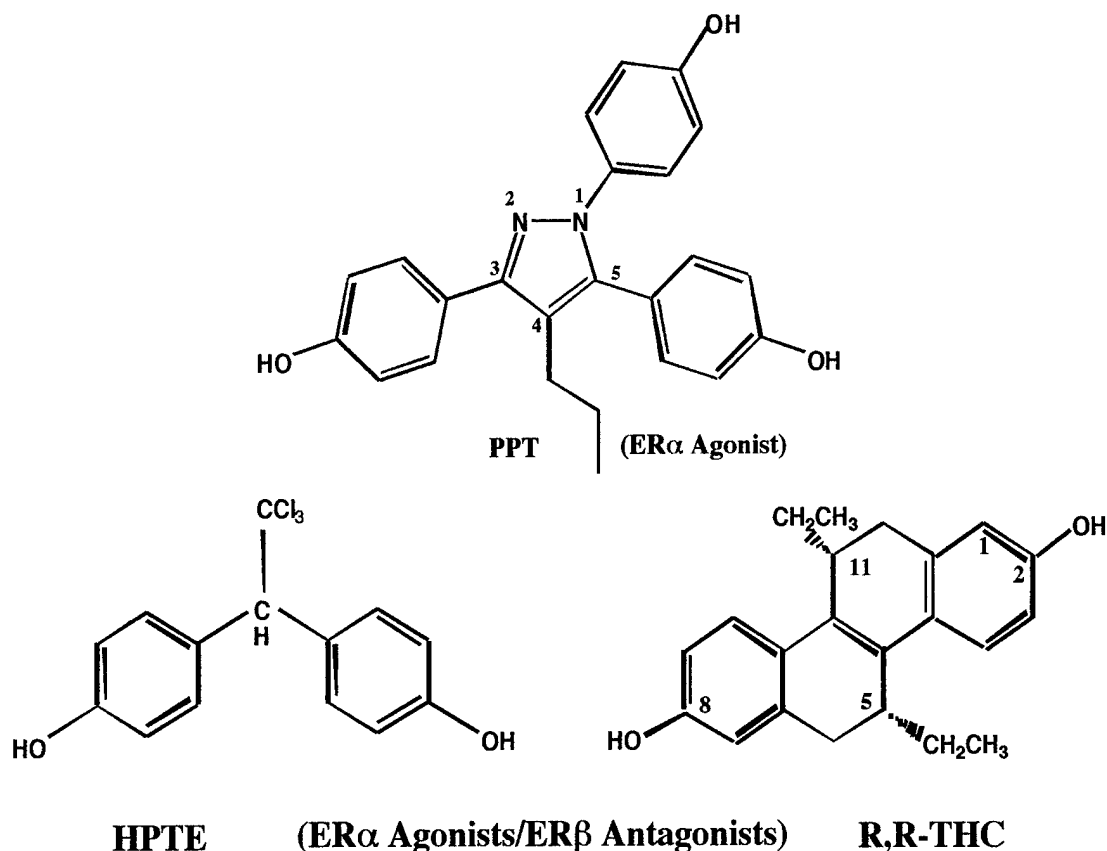


**Figure 5.** Structures of ER $\alpha$ / $\beta$  subtype-selective agonists and antagonists. HPTE = *p*-hydroxyphenyl-trichloroethane. PPT = propylpyrazole triol.

propyl pyrazole triol (**Figures 4B and 5, PPT**), which have been shown to be selective ER $\alpha$  agonists with little or no affinity for ER $\beta$  (16), are unaffected by exchange of these two amino acids. The structural basis for these differences has yet to be determined.

Perhaps these contrasting outcomes are not quite as surprising they appear since we and others have data to show that the two ER subtypes seem to prefer different default conformations (**Appendix, Figure 2B**) and that even for the same ER subtype, structurally similar ligands (e.g. OHT and RAL) can induce unique and subtly different conformations. Therefore, it is very likely that amino acids outside the LBD pocket contribute to ligand discrimination and ER subtype-selective behavior. Additional proof that these subtle conformational differences are real and significant comes from the development of peptides (generated by phage display) that can distinguish between complexes of ER $\alpha$  or ER $\beta$  bound to these ligands (17, 18). For example, a peptide designated  $\alpha/\beta$  V can distinguish between the OHT-ER $\alpha/\beta$  complexes and other SERM-ER complexes, including Ral-ER $\alpha/\beta$  (17). Other peptides (e.g. 7 $\beta$ -16) can selectively recognize GW5638-ER $\alpha/\beta$  compared to other SERM-ER complexes (18). One of our major goals is to understand the structural/molecular basis for these differences. Thus, one approach is to determine the crystallographic structures of ER $\alpha/\beta$  LBD complexes with these ligand-selective peptides. In addition, we will continue to exploit site-directed mutagenesis of both ER subtypes to better define which residues distinguish ER $\alpha$  from ER $\beta$  in response to ligands that have unique activity- and/or ER subtype-selective behavior. This type of

information will be essential for our compound modeling and drug design efforts. We will want to know, for example, the minimum number of amino acids required for ER subtype selection for each of the compounds mentioned above. We will also need to know more about the conformational flexibility of the two ER subtypes and how that flexibility distinguishes between coactivator and corepressor preference.

## KEY RESEARCH ACCOMPLISHMENTS

- Extensive refinement of crystallographic structures of ER $\alpha$  and ER $\beta$  LBDs bound to R,R-THC, an ER $\alpha$  agonist/ER $\beta$  antagonist. New insights into mechanisms of agonism and antagonism revealed.
- Molecular basis of novel concept "passive antagonism", or antagonism without side chains, predicted from structures of ER $\alpha$  and ER $\beta$  LBDs bound to R,R-THC and TIF2/GRIP1 NR box II peptide.
- Novel concept of helix 12 dynamic equilibrium: Positioning of helix 12 is more variable than previously believed and is a key discriminator among diverse agonist- and antagonist-induced conformations of ER $\alpha$  and ER $\beta$ . Hydrophobic cleft in the LBD can accommodate coactivators (agonists), corepressors (antagonists), and/or different orientations of helix 12 in the presence of different antagonists.
- Transcriptionally active conformation of ER LBD requires cooperative participation of ligand, LBD, and coactivator.
- Molecular basis of ER subtype-selective agonism and antagonism predicted from structure of ER $\alpha$  and ER $\beta$  LBDs bound to R,R-THC. R,R-THC binds to the ER $\beta$  LBD without nucleating many of the equivalent cooperative interactions observed in the ER $\alpha$  complex that reflect agonist behavior.
- Preliminary mutagenic analysis of ER $\alpha$  and ER $\beta$  LBDs reveals that ligand-selective  $\alpha$  and  $\beta$  character, especially transcriptional activity, depend on more than the two amino acids that differ in the ligand binding pockets of the two ERs.

## REPORTABLE OUTCOMES

- Manuscripts, Abstracts, Presentations:
  - A manuscript detailing the results reported here was recently submitted to *Nature Structural Biology* for review. It is included in the Appendix.
  - Abstracts for two meetings are included in the Appendix.
  - Presentations (no abstract): Invited speaker at various academic institutions and meetings.
  - Symposium Speaker: Mini-Symposium II, 23<sup>rd</sup> Annual San Antonio Breast Cancer Symposium, San Antonio, TX, 12/00.
- Patents: none
- Degrees obtained with award support: none
- Development of cell lines, etc: none
- Informatics:
  - R,R-THC-ER $\alpha$ / $\beta$  crystallographic coordinates will be deposited in the PDB and will be released upon publication of the structures.
- Funding applied for based on work supported by this award:
  - An R01 proposal (CA89489), "Development and Characterization of Novel SERMs" has been approved for funding by the NCI and funding should begin in August. This work

will complement and extend, but not duplicate, the structural work represented by this DOD award.

- Employment or research opportunities applied for: none

## CONCLUSIONS

The major goal of this investigation is to determine the three-dimensional structures of the two known human estrogen receptors (ER $\alpha$  and ER $\beta$ ) complexed with receptor-selective estrogens and antiestrogens (SERMs). The crystallographic structures of ER $\alpha$  and ER $\beta$  ligand binding domains complexed with *cis*-R,R-diethyl-tetrahydrochrysene-2,8-diol (R,R-THC) have been solved and the data extensively refined, suggesting novel mechanisms by which this compound can act as an ER $\alpha$  agonist and as an ER $\beta$  antagonist. Agonists and antagonists bind at the same site within the core of the ER LBD to induce distinct conformations in the transactivation domain (AF-2), especially in the positioning of helix 12. Previously determined structures of ER $\alpha$  with 4-hydroxytamoxifen (OHT) and diethylstilbestrol (DES) revealed and defined a multipurpose docking site on ER $\alpha$  and ER $\beta$  that can accommodate either helix 12, in the presence of OHT, or one of several co-regulators in the presence of DES. R,R-THC stabilizes a conformation of the ER $\alpha$  LBD that favors coactivator association and a conformation of the ER $\beta$  LBD that prevents coactivator association. A comparison of the two structures, combined with functional data, reveals that R,R-THC does not act on ER $\beta$  through the same mechanisms used by other known ER antagonists. Instead, R,R-THC antagonizes ER $\beta$  through a novel mechanism we term "passive antagonism". Importantly, R,R-THC binds to the ER $\beta$  LBD without nucleating many of the equivalent cooperative interactions observed in the ER $\alpha$  complex that reflect agonist behavior. Paradoxically, the R,R-THC-ER $\beta$  structure is very similar to the structure induced by genistein, which acts as a partial estrogen through both ER subtypes. Clearly, formation of the transcriptionally active conformation of ER LBD requires cooperative participation of ligand, LBD, and coactivator. Ongoing mutagenesis studies should help define the molecular and structural differences that are responsible for these unanticipated results. The passive antagonism mechanism suggests a novel approach to the design of ligands that selectively antagonize the two ER subtypes. Such ligands may have novel therapeutic properties that can be exploited to prevent or treat breast cancer.

So what? It is clear from the various solved structures for ER $\alpha$  and ER $\beta$  bound to diverse SERMs that the resulting ER conformations and ligand pharmacologies are not as simple as previously believed. Rather than just two distinct conformations of ER that reflect agonism or antagonism, it appears that multiple conformations are possible, each of which may mediate a different pharmacology for a particular ligand in a given tissue, such as the breast, uterus, bone, or cardiovascular system. It has become clear that variable antagonism can be achieved both by the presence of bulky side chains and by molecules that lack bulky side chains. Thus, it is important to solve additional structures for ER $\alpha$  and ER $\beta$  complexed with ligands that have been shown to have different tissue-selective pharmacologies, such as GW5638 and ICI 182,780 (Faslodex). In addition, structure-based mutagenic analyses of the two ER subtypes will help define residues that contribute to  $\alpha$  and  $\beta$  activity-selective and subtype-selective behavior. Such information is essential to design compounds that have defined properties. A major goal of this investigation is to characterize and/or design compounds that are useful as chemopreventive agents, especially for breast and uterine cancers. To be useful in a clinical setting, such as

hormone replacement therapy, such compounds must also have the beneficial effects of estrogen, including maintenance of bone density, protection of the cardiovascular system, prevention of hot flashes and perhaps delayed onset of Alzheimer's disease and maintenance of cognitive function. It seems unlikely that a single molecule will have all of these properties. However, it is clear that improved SERMs can be designed and/or discovered. Since most, if not all, of the behavior of the two known ERs is dictated by the conformations induced by diverse natural and synthetic ligands, determination and analysis of the corresponding 3D structures for representative SERMs should be a valuable tool for dissecting underlying molecular mechanisms and for designing new generation compounds. We will therefore continue our efforts to determine and correlate ER-SERM structures with their known biological activities and to understand the unique structural/molecular characteristics that define and differentiate ER $\alpha$  and ER $\beta$ .

## REFERENCES

1. Shiau AK, Barstad D, Loria PM, Cheng L, Kushner PJ, Agard DA, Greene GL 1998 The structural basis of estrogen receptor/coactivator recognition and the antagonism of this interaction by tamoxifen. *Cell* 95:927-37
2. Pike AC, Brzozowski AM, Hubbard RE, Bonn T, Thorsell AG, Engstrom O, Ljunggren J, Gustafsson JA, Carlquist M 1999 Structure of the ligand-binding domain of oestrogen receptor beta in the presence of a partial agonist and a full antagonist. *Embo J* 18:4608-18
3. Pike AC, Brzozowski AM, Walton J, Hubbard RE, Thorsell A, Li Y, Gustafsson J, Carlquist M 2001 Structural Insights into the Mode of Action of a Pure Antiestrogen. *Structure (Camb)* 9:145-53.
4. Fawell SE, White R, Hoare S, Sydenham M, Page M, Parker MG 1990 Inhibition of estrogen receptor-DNA binding by the "pure" antiestrogen ICI 164,384 appears to be mediated by impaired receptor dimerization. *Proc Natl Acad Sci U S A* 87:6883-7.
5. Brzozowski A, Pike A, Dauter Z, Hubbard R, Bonn T, Engstrom O, Ohman L, Greene G, Gustafsson J, Carlquist M 1997 Molecular basis of agonism and antagonism in the oestrogen receptor. *Nature* 389:753-758
6. Barkhem T, Carlsson B, Nilsson Y, Enmark E, Gustafsson J, Nilsson S 1998 Differential response of estrogen receptor alpha and estrogen receptor beta to partial estrogen agonists/antagonists. *Mol Pharmacol* 54:105-12
7. Meyers MJ, Sun J, Carlson KE, Katzenellenbogen BS, Katzenellenbogen JA 1999 Estrogen receptor subtype-selective ligands: asymmetric synthesis and biological evaluation of cis- and trans-5,11-dialkyl- 5,6,11, 12- tetrahydrochrysenes. *J Med Chem* 42:2456-68
8. Sun J, Meyers MJ, Fink BE, Rajendran R, Katzenellenbogen JA, Katzenellenbogen BS 1999 Novel ligands that function as selective estrogens or antiestrogens for estrogen receptor-alpha or estrogen receptor-beta. *Endocrinology* 140:800-4
9. Schultz JR, Tu H, Luk A, Repa JJ, Medina JC, Li L, Schwendner S, Wang S, Thoolen M, Mangelsdorf DJ, Lustig KD, Shan B 2000 Role of LXRs in control of lipogenesis. *Genes Dev* 14:2831-8.
10. Gangloff M, Ruff M, Eiler S, Duclaud S, Wurtz JM, Moras D 2001 Crystal structure of a mutant hERalpha ligand-binding domain reveals key structural features for the mechanism of partial agonism. *J Biol Chem* 276:15059-65.
11. Steinmetz AC, Renaud JP, Moras D 2001 Binding of ligands and activation of transcription by nuclear receptors. *Annu Rev Biophys Biomol Struct* 30:329-59.

12. Singh SM, Gauthier S, Labrie F 2000 Androgen receptor antagonists (antiandrogens): structure-activity relationships. *Curr Med Chem* 7:211-47.
13. Greene GL, Gilna P, Waterfield M, Baker A, Hort Y, Shine J 1986 Sequence and expression of human estrogen receptor complementary DNA. *Science* 231:1150-4
14. Mosselman S, Polman J, Dijkema R 1996 ER beta: identification and characterization of a novel human estrogen receptor. *FEBS Lett* 392:49-53
15. Gaido KW, Leonard LS, Maness SC, Hall JM, McDonnell DP, Saville B, Safe S 1999 Differential interaction of the methoxychlor metabolite 2,2-bis-(p-hydroxyphenyl)-1,1,1-trichloroethane with estrogen receptors alpha and beta. *Endocrinology* 140:5746-53.
16. Stauffer SR, Huang Y, Coletta CJ, Tedesco R, Katzenellenbogen JA 2001 Estrogen pyrazoles: defining the pyrazole core structure and the orientation of substituents in the ligand binding pocket of the estrogen receptor. *Bioorg Med Chem* 9:141-50.
17. Paige LA, Christensen DJ, Gron H, Norris JD, Gottlin EB, Padilla KM, Chang CY, Ballas LM, Hamilton PT, McDonnell DP, Fowlkes DM 1999 Estrogen receptor (ER) modulators each induce distinct conformational changes in ER alpha and ER beta. *Proc Natl Acad Sci U S A* 96:3999-4004
18. Connor CE, Norris JD, Broadwater G, Willson TM, Gottardis MM, Dewhirst MW, McDonnell DP 2001 Circumventing tamoxifen resistance in breast cancers using antiestrogens that induce unique conformational changes in the estrogen receptor. *Cancer Res* 61:2917-22.



**ANNUAL REPORT FOR Award Number DAMD17-99-1-9120**

**APPENDIX**

**Manuscript submitted to *Nature Structural Biology*:**

Andrew K. Shiau, Danielle Barstad, James T. Radek, Marvin J. Meyers, Benita S. Katzenellenbogen, John A. Katzenellenbogen, David A. Agard, and Geoffrey L. Greene.  
Structural Characterization of an Estrogen Receptor  $\alpha$  Agonist/Estrogen Receptor  $\beta$  Antagonist Reveals a Novel Mode of Receptor Antagonism.

**Selected abstracts of presentations at national or international meetings:**

1. 14<sup>th</sup> International Symposium of the Journal of Steroid Biochemistry & Molecular Biology, Quebec City, Canada, 6/00.
2. 14<sup>th</sup> Annual Symposium on the Long-Term Effects of Estrogen Deprivation, Telluride, Colorado, 7/00.
3. Hormones and Cancer 2000, Port Douglas, Australia, 11/00.
4. LAMPOSIUM 2001, Cincinnati, Ohio, 3/01.
5. EMBO Workshop on Nuclear Receptor Structure and Function, Erice, Sicily, Italy, 5/01.

# **Structural Characterization of an Estrogen Receptor $\alpha$ Agonist/Estrogen Receptor $\beta$ Antagonist Reveals a Novel Mode of Receptor Antagonism**

Andrew K. Shiau<sup>1,2</sup>, Danielle Barstad<sup>3</sup>, James T. Radek<sup>3</sup>, Marvin J. Meyers<sup>4</sup>,  
Benita S. Katzenellenbogen<sup>5</sup>, John A. Katzenellenbogen<sup>4</sup>, David A. Agard<sup>1</sup>, and  
Geoffrey L. Greene<sup>3</sup>

<sup>1</sup> The Howard Hughes Medical Institute and Department of Biochemistry and Biophysics  
University of California  
San Francisco, California 94143

<sup>2</sup> Tularik Inc.  
Two Corporate Drive  
South San Francisco, California 94080

<sup>3</sup> The Ben May Institute for Cancer Research and Department of Biochemistry and Molecular Biology  
University of Chicago  
Chicago, Illinois 60637

<sup>4</sup> Department of Chemistry  
University of Illinois  
Urbana, Illinois 61801

<sup>5</sup> Departments of Molecular and Integrative Physiology and Cell and Structural Biology  
University of Illinois  
Urbana, Illinois 61801

Correspondence should be addressed to A.K.S.  
email: [ashiau@tularik.com](mailto:ashiau@tularik.com)  
Telephone: (650) 825-7564  
Fax: (650) 825-7318

Nuclear receptor (NR) ligands regulate the transcriptional activity of NRs by stabilizing distinct conformations of the ligand binding domains (LBDs) of their cognate receptors. NR agonists favor LBD conformations that allow NRs to interact with transcriptional coactivator proteins, essential mediators of the transcriptional activation process. By contrast, NR antagonists favor LBD conformations that inhibit the interaction of NRs with coactivators. The R,R enantiomer of 5,11-*cis*-diethyl-5,6,11,12-tetrahydrochrysene-2,8-diol (THC) was recently identified as an estrogen receptor (ER) ligand that differentially affects the transcriptional activity of the two ER subtypes; THC functions as an ER $\alpha$  agonist and as an ER $\beta$  antagonist. We have determined the crystal structure of the ER $\alpha$  LBD bound to both THC and a peptide containing the NR box II region of the coactivator GRIP1 and that of the ER $\beta$  LBD bound to THC. THC stabilizes a conformation of the ER $\alpha$  LBD that favors coactivator association and a conformation of the ER $\beta$  LBD that prevents coactivator association. A comparison of the two structures, combined with functional data, reveals that THC does not act on ER $\beta$  through the same mechanisms used by other known ER antagonists. Instead, THC antagonizes ER $\beta$  through a novel mechanism we term "passive antagonism".

Estrogens play central roles in the differentiation, development, and homeostasis of a wide variety of vertebrate tissues<sup>1</sup>. Currently, a number of estrogenic compounds are being used to regulate human fertility and to treat human diseases, including osteoporosis, cardiovascular disease, and breast cancer (ref). The physiological effects of both endogenous and synthetic estrogens are mediated by the estrogen receptors (ERs), ER $\alpha$  and ER $\beta$ , members of the nuclear receptor (NR) superfamily of ligand-regulated transcription factors. The two ERs have overlapping but distinct tissues distribution patterns *in vivo* and distinct activation profiles at both classical and complex promoter elements (ref). Hence, it is unclear how ER $\alpha$  and ER $\beta$  individually contribute to the effects of known estrogens. Ligands that act differentially on ER $\alpha$  and ER $\beta$  would be potentially

valuable both as tools to dissect the biological roles of the two ERs and as novel therapeutics with pharmacological properties distinct from existing drugs.

In a search for ER subtype-selective ligands, the R,R enantiomer of 5,11-*cis*-diethyl-5,6,11,12-tetrahydrochrysene-2,8-diol (THC) (Figure 1A) was identified as a compound with a significant affinity preference for ER $\beta$  over ER $\alpha$  ( $K_d = 1.3$  nM and 0.2 nM for ER $\alpha$  and ER $\beta$ , respectively), and profoundly different activation profiles on the two ERs<sup>2,3</sup>. THC functions as an agonist on ER $\alpha$  with an  $EC_{50} \sim 3$  nM but has no effect on the transcriptional activity of ER $\beta$ . Instead, this compound potently antagonizes the effects of the endogenous estrogen, 17 $\beta$ -estradiol (E2), on ER $\beta$  with an  $IC_{50} < 10$  nM<sup>2,3</sup>. Consistent with these subtype-specific effects on transcriptional activation, THC also differentially affects the two ERs in protease protection and coactivator recruitment assays<sup>4</sup>. However, the molecular basis of the subtype-dependent behavior of the compound is still not understood. Here we describe structural and further functional characterization of the effects of THC on ER $\alpha$  and ER $\beta$ . These studies indicate that THC exerts its effects on the transcriptional activity of the two ERs by differentially affecting the structures of the two receptors and that THC antagonizes ER $\beta$  through a mechanism distinct from those used by other known ER antagonists.

### Subtype-selective Transcriptional Effects of THC

The transcriptional activity of ER $\alpha$  results from at least two functionally separable transcriptional activation functions (AFs), AF-1 within the N terminus and AF-2 within the C-terminal ligand binding domain (LBD)<sup>5,6</sup>. By contrast, the transcriptional activity of ER $\beta$  is largely dominated by that of AF-2 within its LBD<sup>7,8</sup>. AF-1 activity is regulated by growth factor-inducible phosphorylation by MAP kinases<sup>9</sup>, while AF-2 activity is regulated by the binding of ligands (**ref**). Pure agonists, such as E2 and the synthetic nonsteroidal estrogen diethylstilbestrol (DES), trigger AF-2 activity while pure antagonists, such as ICI 164,384 (ICI), and mixed-

function partial agonist/antagonists, such as 4-hydroxytamoxifen (OHT) and raloxifene (RAL), block AF-2 activity (Figure 1A) (ref). AF-1 and AF-2 may contribute independently, additively, or synergistically to the activity of ER $\alpha$  depending on the ligand and promoter context (ref). As a result, the agonist activity of THC may arise from the stimulation of AF-1 and/or AF-2.

To determine if THC regulates ER $\alpha$  AF-2 activity, a series of transcriptional assays were performed using fusions between the DNA binding domain (DBD) of the yeast transcriptional activator, GAL4, and the ER $\alpha$  LBD. For comparison, equivalent assays were performed using a similar fusion between the GAL4 DBD and the ER $\beta$  LBD. E2 stimulates the transcriptional activity of both the ER $\alpha$  and ER $\beta$  LBD chimeras (Figure 1B). By contrast, THC stimulates the transcriptional activity of the ER $\alpha$  LBD fusion (albeit to a lesser degree than E2) but has no effect on the transcriptional activity of the ER $\beta$  LBD chimera (Figure 1B). Consistent with its effects on full-length ER $\beta$ <sup>2,3</sup>, THC also antagonizes the effects of E2 on the ER $\beta$  LBD chimera (data not shown). Thus, THC affects the AF-2-derived transcriptional activities of the two ERs in a subtype-selective manner.

### **Overall Structures of the THC-ER LBD Complexes**

Recent structural studies indicate that NR ligands regulate AF-2 activity by modulating the structure of NR LBDs. NR ligands bind to their cognate receptors within a hydrophobic pocket formed within the core of the narrower or “lower” half of the LBD. The binding of an AF-2 agonist to an NR LBD triggers the repositioning of the most C-terminal helix of the LBD, helix 12, such that it lies across the entrance to the ligand binding pocket, sealing in the agonist<sup>10</sup>. This conformation of the LBD allows the receptor to interact with a class of proteins known as transcriptional coactivators, which enhance ligand-dependent transcription of NRs<sup>11</sup>. Members of the p160 family of coactivators<sup>11</sup>, including SRC-1/NCoA1, GRIP1/TIF2/NCoA2, and p/CIP/RAC3/ACTR/AIB1, recognize agonist-bound NR LBDs via short sequence motifs, LXXLL (where L is leucine and X is any amino acid) called NR

boxes<sup>12-15</sup>. These NR boxes form amphipathic  $\alpha$ -helices which recognize a hydrophobic groove on the surface of an agonist-bound LBD formed by residues from helices 3, 4, 5, and 12<sup>16-19</sup>.

By contrast, NR AF-2 antagonists stabilize alternative LBD conformations that sterically preclude coactivator recognition. The structures of the BMS614-retinoic acid receptor  $\alpha$ <sup>20</sup>, OHT-ER $\alpha$ <sup>19</sup>, RAL-ER $\alpha$ <sup>21</sup>, RAL-ER $\beta$ <sup>22</sup>, and ICI-ER $\beta$  LBD<sup>23</sup> complexes reveal that certain portions of these compounds, termed extensions or side chains, cannot be contained within the ligand binding pocket. Instead, these side chains project out of the entrance to the binding pocket, which is covered by helix 12 in the agonist-bound LBD structures. Hence, helix 12 is precluded from adopting the "agonist-bound" conformation. In addition, the structures of the BMS614, OHT, and RAL complexes show that these antagonists also induce structural distortions in and around the binding pocket, that favor an extended conformation of the segment of peptide backbone which forms the C-terminal end of helix 11 in the agonist-bound structures. This "unraveling" of helix 11 allows helix 12 to reach the static region of the coactivator recognition groove formed by helices 3, 4, and 5 and occlude the recognition groove by mimicking the interactions of the NR box with the LBD<sup>19-22</sup>. ICI affects helix 12 positioning in a different manner. In its complex with the ER $\beta$  LBD, the terminal n-butyl moiety of the ICI side chain embeds itself in the recognition groove, preventing both coactivator binding and the helix 12 conformation observed in the other antagonist complexes. As a result, helix 12 is completely disordered in this complex<sup>23</sup>.

Curiously, the recent structure of the ER $\beta$  LBD bound to the ER $\beta$  partial agonist genistein (GEN) reveals that ligand binding may support yet a third conformation of helix 12<sup>22</sup>. Helix 12 is bound over the ligand binding pocket in a position that only partially occludes the coactivator recognition surface. The functional significance of this conformation of the LBD is unclear.

These structural data and the behavior of THC in transactivation assays suggest a striking prediction: the same ligand, THC, should be able to both stabilize a

conformation of the ER $\alpha$  LBD that favors coactivator binding and a conformation of the ER $\beta$  LBD that precludes coactivator binding. Notably, THC, unlike all other known ER antagonists, such as OHT, RAL, and ICI, lacks a bulky extension or side chain (Figure 1A), so THC must act on ER $\beta$  by fundamentally different mechanisms than these other antagonists.

In order to verify this prediction, crystals of the ER $\alpha$  LBD bound to both THC and a peptide derived from the second NR Box of the coactivator GRIP1 and of the ER $\beta$  LBD bound to THC were grown and both structures determined by molecular replacement. The ER $\alpha$  complex structure has been refined to a crystallographic R factor of 20.3% ( $R_{\text{free}} = 24.2\%$ ) using data to 1.95 Å and the ER $\beta$  complex structure has been refined to a crystallographic R factor of 26.5% ( $R_{\text{free}} = 30.4\%$ ) using data to 2.85 Å (Table 1 and Figure 4A).

When bound to THC, the ER $\alpha$  LBD adopts the same conformation as it does when it is bound to the full agonists E2 and DES (Figure 2A)<sup>19,21</sup>. The LBD is a wedge-shaped molecule composed of a small beta hairpin and eleven to twelve helices arranged in three layers. Helix 12 adopts the agonist-bound conformation in the THC-ER $\alpha$  LBD complex; helix 12 packs against helices 3, 5, 6, and 11, covering the entrance to the ligand binding cavity. THC is completely enveloped by the binding cavity within the lower subdomain of the LBD formed by residues from helices 3, 6, 7, 8, 11, and 12 and the beta hairpin (Figure 2A). As in the DES-ER $\alpha$  LBD-GRIP1 peptide complex<sup>19</sup>, the coactivator peptide is bound in an  $\alpha$ -helical conformation to a hydrophobic groove on the surface of the LBD formed by residues from helices 3, 4, 5, and 12 (Figure 2A).

As described previously, the ER $\beta$  LBD shares the same overall fold as the ER $\alpha$  LBD (Figure 2A)<sup>22</sup>. And like the ER $\alpha$  LBD, the ER $\beta$  LBD recognizes THC with a ligand binding pocket located within its lower subdomain. However, the binding of THC to the ER $\beta$  LBD does not stabilize the agonist-bound conformation of helix 12

(Figure 2A). Neither is helix 12 bound to the portion of the coactivator recognition groove formed by helices 3, 4, and 5 as it is in the OHT-ER $\alpha$  LBD<sup>19</sup>, RAL-ER $\alpha$  LBD<sup>21</sup>, and RAL-ER $\beta$  LBD<sup>22</sup> complexes (Figure 2B), nor is it disordered as it is in the ICI-ER $\beta$  LBD complex<sup>23</sup>. Instead, helix 12 in the THC-ER $\beta$  LBD complex interacts with the rest of the LBD in a manner most like that observed in the GEN-ER $\beta$  LBD complex (Figure 2B)<sup>22</sup>.

Helix 12 is positioned similarly, and of comparable length (residues 487 to 498 in the THC complex and residues 487 to 497 in the GEN complex<sup>22</sup>) in the two structures (Figure 2B). At the N-terminal end of helix 12, the side chain of Val 487 (which packs against the side chains of Leu 306 and Trp 335 in the THC complex) is inserted into the entrance to the ligand binding pocket formed by helices 3, 5/6, and 11 in both complexes. This causes the C-terminal end of helix 12 to project away from the rest of the LBD. As a result, the side chains of Leu 491, Met 494, and Leu 495, which mimic the interactions of the three NR box leucines with the static region of the coactivator recognition groove in the RAL-ER $\beta$  LBD complex<sup>22</sup>, only partially occlude the coactivator binding site in the GEN<sup>22</sup> and THC complexes. In the THC complex, the side chain of Leu 491 packs against that of Trp 335. The side chain of Met 494 packs against those of residues on helix 3 (Asp 303, Leu 306, and Val 307) and the side chain of Leu 495 is embedded within the coactivator binding groove and packs against the side chains of Ile 310, Val 328, Leu 331, and Glu 332.

### **Ligands and Helix 12 Positioning**

The conformation of the ER $\beta$  LBD observed in both the THC and GEN complexes should be incapable of interacting with coactivators and, hence, transcriptionally silent for two reasons. The residues from helix 12 (Leu 490, Glu 493, and Met 494) that are predicted to form part of the coactivator recognition surface are inappropriately positioned, and helix 12 itself is bound such that it partially occludes the static region of the coactivator binding surface formed by residues from helices 3, 4, and 5. Yet, GEN and THC clearly exhibit different activities on ER $\beta$  in



mammalian cells; GEN acts as a partial agonist<sup>8</sup> and THC acts as a pure antagonist<sup>2,3</sup>. How can the similarity of the two structures be reconciled with the different activities of these compounds in transcriptional assays?

The simplest model that explains these and other data is based on two suppositions (Figure 3A). First, helix 12 in the unliganded ER $\beta$  LBD is in equilibrium between the THC/GEN-bound conformation, which precludes coactivator association, and the agonist-bound conformation seen in the E2- and DES-ER $\alpha$  LBD structures, which favors coactivator association (with the “inactive” THC/GEN-bound conformation being heavily favored). Second, rather than stabilizing a single static conformation of helix 12, ligands serve to shift the balance of this equilibrium.

According to this model, helix 12 in the unliganded or apo-ER $\beta$  LBD, although largely in a transcriptionally silent conformation, may also adopt a transcriptionally active one (Figure 3A). Hence, the low but detectable constitutive AF-2-derived transcriptional activity of the apo-LBD would result from the modest but significant affinity of the apo-LBD for coactivator<sup>8</sup>. Full agonists, such as E2 and DES, shift the helix 12 conformational equilibrium heavily in favor of the “active” conformation, and stimulate AF-2 activity by increasing the affinity of the LBD for coactivator (Figure 3A). Because they are incapable of shifting the equilibrium in favor of the active conformation to the same extent as full agonists, partial agonists, such as GEN, are only able to incrementally increase the affinity of the receptor for coactivator and, hence, activate AF-2 less efficiently than full agonists (Figure 3A). GEN binding should allow the ER $\beta$  LBD to sample both inactive and active conformations of helix 12 (possibly to comparable extents). The fact that the inactive THC/GEN-bound conformation is observed in the crystal structure may reflect the true bias of the equilibrium in solution or it may be the result of the influence of the crystallization conditions on the equilibrium.

In principle, THC could antagonize receptor activity by shifting equilibrium in favor of the inactive THC/GEN-bound conformation (Figure 3A). If THC binding

forces the receptor to favor this conformation even more than it does in the absence of ligand, the THC-receptor complex would be expected to have an even lower affinity for coactivator than the unliganded receptor. This would be consistent with the absence of transcriptional activity of the THC-ER $\beta$  complex and the conformation of helix 12 observed in the crystal.

The helix 12 conformational equilibrium would be difficult to observe directly. Nonetheless, the mechanisms of the various ligands, inferred from the model described above, suggest a testable hypothesis: the binding of different ligands should modulate the affinity of the ER $\beta$  LBD for coactivator such that E2-LBD ~ DES-LBD > GEN-LBD > apo-LBD > THC-LBD. The affinities of various ligand-ER $\beta$  LBD complexes for an LXXLL motif-containing peptide were directly measured using a fluorescence polarization-based binding assay (Figure 3B)<sup>24</sup>. The full agonist complexes bind the peptide approximately 1.5-fold more tightly than the GEN complex ( $K_d$ [E2] = 0.36  $\mu$ M and  $K_d$ [DES] = 0.41  $\mu$ M versus  $K_d$ [GEN] = 0.58  $\mu$ M). In addition, the GEN complex binds the peptide more tightly than the unliganded receptor ( $K_d$ [apo] = 2.1  $\mu$ M), whereas the THC complex ( $K_d$ [THC] = 3.7  $\mu$ M) binds the peptide significantly weaker than the unliganded receptor. Thus, these and other previously described biochemical data are entirely consistent with the described helix 12 conformational equilibrium model. Furthermore, recent mutational and crystallographic data suggest that the positioning of helix 12 in ER $\alpha$ <sup>25</sup> and other NRs<sup>10</sup> is also dictated by a ligand-sensitive conformational equilibrium.

### **THC Interaction with the ER $\alpha$ and ER $\beta$ LBDs**

THC binding stabilizes a transcriptionally active conformation of the ER $\alpha$  LBD and a transcriptionally inactive one of the ER $\beta$  LBD. The conformation of an NR LBD stabilized by a particular ligand is the direct structural consequence of the interactions formed between that ligand and the binding pocket of that protein.

Consistent with these ideas, THC interacts with the ligand binding pockets of the two ERs in substantially different ways.

The ER $\alpha$  LBD recognizes THC much as it does the agonists, E2<sup>21,25,26</sup> and DES<sup>19</sup> (Figures 4B and 4C). The A ring of THC is bound in approximately the same position as the A rings of E2 and DES near helices 3 and 6. The A ring itself interacts with the side chains of Ala 350, Leu 387, Leu 391, and Phe 404 and the A ring phenolic hydroxyl forms hydrogen bonds to the side chain carboxylate of Glu 353, to the guanidinium group of Arg 394, and to a buried water molecule. The A' ring of THC is bound by the opposite end of the binding pocket near helices 7, 8, and 11 which binds the D ring of E2 and the A' ring of DES. The A' ring forms van der Waals contacts with Met 421, Ile 424, Gly 521, His 524, and Leu 525, and the phenolic hydroxyl hydrogen bonds with the side chain imidazole of His 524.

Although THC, E2, and DES form many of the same interactions with ER $\alpha$ , the three ligands differ in their ability to fill the binding pocket. In the E2 complex, there are unoccupied cavities adjacent to the  $\alpha$  face of the B ring and the  $\beta$  face of the C ring of E2<sup>21,25,26</sup>. DES is able to fill both of these cavities with its two ethyl groups<sup>19</sup>. One of the ethyl groups of THC fills the B ring  $\alpha$  face cavity by forming packing interactions with Leu 391, Phe 404, Met 421, Phe 425, and Leu 428 (Figures 4B and 4C). However, due to the *cis* stereochemistry of the molecule, the other ethyl group of THC points towards the  $\alpha$  face, instead of the  $\beta$  face, of the C ring region of the binding pocket. Therefore, this ethyl group is unable to fill the cavity near the C ring, and instead packs against the side chains of Leu 346 and Met 421 (Figures 4B and 4C). In order to accommodate these additional interactions, the THC scaffold is tilted approximately 10° away from the floor of the binding pocket (and Leu 346) relative to the plane of the E2 scaffold. This suboptimal alignment may result in the reduced agonist activity of THC (relative to E2) on ER $\alpha$ . This idea is supported by the observation that the *trans* analog of THC, whose ethyl groups should be positioned like those of DES, acts as a full agonist on ER $\alpha$ <sup>2</sup>.

THC binds to the two ERs in a grossly similar manner (Figure 4C). However, the two ethyl groups of THC adopts significantly different conformations in the two complexes. Whereas the two ethyl groups are rotated underneath the tetrahydrochrysene scaffold in the ER $\alpha$  complex, they are rotated outwards away from the body of THC in the ER $\beta$  complex (Figures 4A and 4C). As it does in the ER $\alpha$  complex, one ethyl group fills the  $\alpha$  face B ring cavity in the ER $\beta$  complex and forms nonpolar contacts with Leu 343, Phe 356, and Leu 380 (Figures 4B and 4C). But, in order to accommodate its extended conformation, the tetrahydrochrysene scaffold is displaced both towards the entrance of the binding pocket (near helices 3, 6, and 11) and away from the floor of the binding pocket relative to its position in the ER $\alpha$  complex (Figure 4C).

This displacement significantly affects the interaction of THC with the ER $\beta$  ligand binding pocket in several ways. First, it allows the other ethyl group not only to pack against Leu 298 (equivalent to Leu 346 in ER $\alpha$ ), but also to Thr 299 at the entrance to the binding pocket (Figure 4B). Even more importantly, because of its altered positioning, the tetrahydrochrysene scaffold of THC is only able to interact with a subset of the equivalent ER $\beta$  LBD residues that it interacts with in the ER $\alpha$  complex (Figures 4B and 4C). The A ring of THC is bound in the region of the ER $\beta$  binding pocket near helices 3 and 6, as it is in the ER $\alpha$  complex. But in the ER $\beta$  complex the THC A ring only interacts with three (Ala 302, Leu 339, and Phe 356, equivalent to Ala 350, Leu 387, and Phe 404, respectively) of the four residues that it packs against in the ER $\alpha$  complex. In the ER $\alpha$  complex, the phenolic A ring hydroxyl forms hydrogen bonds with the side chains of Glu 353, Arg 394, and a buried water molecule. Because it is bound somewhat more distantly from the equivalent residues (Glu 305 and Arg 346) in the ER $\beta$  complex, the A ring hydroxyl is unable to interact with the equivalent buried water and only forms hydrogen bonds to the side chains of Glu 305 and Arg 346. At the opposite end the the pocket, the A' ring of THC in the ER $\beta$  complex packs against three (Gly 472, His 475, and Leu

476, equivalent to Gly 521, His 524, and Leu 525, respectively) of the five residues it interacts with in the ER $\alpha$  complex. Because it is displaced by approximately 1 Å relative its location in the ER $\alpha$  complex, the A' ring phenolic hydroxyl is unable to hydrogen bond with the imidazole of His 475. Instead, the A' ring hydroxyl forms a weak hydrogen bond to the carbonyl of Gly 472.

When they bind to ER $\alpha$  (and presumably ER $\beta$ ), ER agonists favor the agonist-bound conformation of helix 12, but they do so indirectly<sup>19,21</sup>. An ER agonist forms hydrogen bonds and van der Waals contacts with residues from helices 3, 5, 6, 11 and the beta turn, stabilizing these residues in conformations that allow them to interact with the ligand, with each other, and with other residues in and around the binding pocket. The formation of this series of cooperative interactions orients residues from helices 3, 5, 6, and 11 such that they create a predominantly hydrophobic binding surface for helix 12. This results in a shift in the helix 12 conformational equilibrium towards the agonist-bound conformation. From a structural standpoint, THC acts as an ER $\alpha$  agonist. When bound to ER $\alpha$ , THC fulfills all of the hydrogen bonding and nonpolar interactions observed in the E2 and DES complexes that nucleate the multiple cooperative interactions in and around the binding pocket that favor the agonist-bound conformation of helix 12.

By these criteria, THC does not behave as an ER $\beta$  agonist. As described above, THC binds to ER $\beta$  without interacting with several residues that it contacts in ER $\alpha$ , and by forming alternative hydrogen bonds and additional packing contacts not observed in the ER $\alpha$  complex (Figures 4B and 4C). Hence, THC is able to bind to the ER $\beta$  LBD without nucleating many of the equivalent cooperative interactions observed in the ER $\alpha$  complex. For example, in the ER $\alpha$  complex the side chain of Met 528 packs against the side chains of His 524 and Met 343, stabilizing the helical conformation of the flanking residues. Because THC binding favors alternative conformations of His 475 and Met 295 (equivalent to His 524 and Met 343, respectively), the side chain of Met 479 (equivalent to Met 528) is completely

disordered in the ER $\beta$  complex. In fact, by stabilizing conformations of binding pocket residues that prevent their interaction, THC binding should actually disfavor the equilibrium to the agonist-bound conformation of helix 12 (Figures 3A and 3B).

What differences between the two ERs allow THC to stabilize these distinct arrangements of ligand binding pocket residues? There are only two binding pocket residues which are not identical in the two subtypes: Leu 384 (from helix 5/6) and Met 421 (from helix 8) in ER $\alpha$ , which are equivalent to Met 336 and Ile 373, respectively, in ER $\beta$ <sup>27-29</sup>. These two residue pairs are similarly positioned on opposite faces of THC in their respective complexes. In the ER $\alpha$  complex, Leu 384 and Met 421 form several nonpolar contacts with THC (Figures 4B and 4C). By contrast, only Met 336 interacts with THC in the ER $\beta$  complex (Figures 4B and 4C).

Modeling suggests that Met 336 and Ile 373 would adopt both different positions and different conformations (relative to their positions in the THC-ER $\beta$  complex) in the agonist-bound conformation of the ER $\beta$  LBD (Figure 5). There is currently no known structure of ER $\beta$  bound to a full agonist. However, given its similarity to the E2-ER $\alpha$ <sup>21</sup> and DES-ER $\alpha$  LBD complexes<sup>19</sup> (outside of helix 12 and the loop connecting helices 11 and 12), the GEN-ER $\beta$  LBD complex<sup>22</sup> may serve as the basis for a model of the agonist-bound conformation of the ER $\beta$  LBD. In order for the A' ring region of THC to fit between the side chains of Met 336 and Ile 373 (in this model), THC would need to be positioned lower in the ER $\beta$  binding pocket relative to its location in the ER $\alpha$  binding pocket. This is because the side chain of Met 336 is larger than that of Leu 384, and conversely the side chain of Ile 373 is smaller than that of Met 421. This lower position should be highly unfavorable because it would result in a steric clash between both atoms of one of the THC ethyl groups with the side chain of Leu 298 at the floor of the pocket (Figure 5). To apparently avoid this unfavorable interaction, THC binds in the alternative mode observed in the crystal. Consistent with this hypothesis, the dimethyl analog of

THC, which should be less sterically hindered from adopting the lower position, acts as a weak ER $\beta$  partial agonist<sup>2</sup>.

Because the conformational effects of ligand binding are cooperative in nature, residues that lie outside the binding pocket may also play roles the subtype-selective effects of THC. Nevertheless, preliminary mutagenesis results indicate that Leu 384/Met 336 and Met 421/Ile 373 do contribute to these effects (unpublished results).

### **“Passive” Antagonism - Antagonism Without Side Chains**

The positioning of the side chains of OHT, RAL, and ICI directly or "actively" preclude the agonist-bound conformation of helix 12 by steric hindrance. Hence, we define their common mechanism of action as "active antagonism". Clearly, THC does not have a side chain (Figure 1A), and in its complex with ER $\beta$ , helix 12 is not sterically precluded from adopting the agonist-bound conformation as it is in the other antagonist complexes (Figures 2A and 4C). Instead, THC antagonizes ER $\beta$  by stabilizing key ligand binding pocket residues in noninteracting conformations, and disfavoring the equilibrium to the agonist-bound conformation of helix 12. Thus, we term the mechanism of antagonism of THC as “passive antagonism”.

Passive antagonism may not be unique to THC and ER $\beta$ . There are many examples of NR ligands, which act as antagonists even though they are smaller than the endogenous agonists of these NRs. The synthetic androgen receptor antagonist, flutamide, is comparable in size to testosterone, and does not possess an obvious moiety that would act as an antagonist side chain<sup>30</sup>. Similarly, progesterone is smaller than aldosterone, yet it is a high affinity antagonist of the mineralocorticoid receptor<sup>31,32</sup>.

Many NRs have multiple subtypes, that possess distinct expression patterns and that regulate distinct target genes (ref). Antagonists generated through the addition of bulky side chains to agonist scaffolds are limited to being antagonistic on one or more subtypes of a particular NR. The passive antagonism mechanism, as revealed here through direct comparison of the two THC-ER LBD complexes,

suggests a new approach to achieving NR antagonism. Compounds could be designed to selectively stabilize the inactive conformations of certain NR subtypes and the active conformations of others. Such ligands may exert novel biological and therapeutic effects.



## Methods

### Transcriptional Activation Assays

The GAL4 DBD/human ER $\alpha$  LBD fusion expression plasmid, pDB-GAL4 ER $\alpha$  LBD (**ref**), the luciferase reporter plasmid, GALRE5-e1b-TATA-Luc (**ref**), (both provided by P. Webb), and the GRIP1 expression plasmid, pSG5 GRIP1<sup>14</sup>, (provided by M. Stallcup) have been described. The GAL4 DBD/human ER $\beta$  LBD fusion expression plasmid (pBD-GAL4 ER $\beta$  LBD) was constructed by inserting a fragment encoding the human ER $\beta$  LBD (residues 256-505) into pBD-GAL4 (Stratagene) by standard methods.

Transient transfections were performed using an activated dendrimer transfection reagent (SuperFect; Qiagen). MDA-MB-231 breast cancer cells were seeded into 48-well tissue culture plates (Falcon, Becton Dickinson) at  $1.5 \times 10^4$  cells/well in phenol red-free DMEM containing 10% heat-inactivated and charcoal-stripped fetal calf serum (DMEM-FCS; HyClone Laboratories), and incubated for 24 hrs at 37 °C in 5% CO<sub>2</sub>. Cells were washed in Dulbecco's phosphate buffered saline (DPBS) prior to transfection. The receptor expression plasmids (20 ng/well), the coactivator expression plasmid (200 ng/well), the reporter plasmid (750 ng/well), and the pRL-TK *renilla* luciferase control plasmid (Promega) (75 ng/well) were incubated with the Superfect reagent (at a ratio of 1  $\mu$ g of total plasmids per 2  $\mu$ L of reagent) in serum-free DMEM for 10 min at ambient temperature. The samples were then diluted six-fold in DMEM-FCS and incubated (0.3 mL/well) for 2.5 hrs at 37 °C in 5% CO<sub>2</sub>. The transfection media was removed, and the cells were washed with DPBS and incubated in DMEM-FCS with the appropriate ligand for 24 hrs at 37 °C in 5% CO<sub>2</sub>. After removal of the media, the cells were again washed in DPBS and lysed with 50  $\mu$ L/well of passive lysis buffer (Promega). Samples (5  $\mu$ L aliquots) were assayed for firefly luciferase and *renilla* luciferase activity using the Dual-Luciferase Reporter 1000 Assay System (25  $\mu$ L each of the firefly and *renilla* luciferase substrates; Promega).

### Protein Expression and Purification

The human ER $\alpha$  LBD (residues 297 to 554) was expressed, carboxymethylated, and purified as previously described<sup>19</sup>. For crystallographic studies, the human ER $\beta$  LBD (residues 256 to 505) was expressed as a N-terminally hexahistidine-tagged fusion protein in BL21(DE3)pLysS cells using the pET expression system (Novagen). Bacterial lysates were applied to an estradiol-Sepharose column<sup>33</sup> and the bound ER $\beta$  LBD was carboxymethylated with 20 mM iodoacetic acid<sup>34</sup>. Protein was eluted with 30  $\mu$ M THC in ~50 ml of 20 mM Tris·Cl, 1M Urea, and 10% DMF pH 8.1. The ER $\beta$  LBD was further purified by ion exchange chromatography (Resource Q, Pharmacia). Protein samples were analyzed by SDS-PAGE, native PAGE, and electrospray ionization mass spectrometry. For biochemical studies, residues 214 to 530 of human ER $\beta$  were expressed as a fusion with glutathione-S-transferase (GST) in BL21 cells using the pGEX expression system (Pharmacia). The GST fusion protein was bound to glutathione Sepharose 4 Fast Flow (Pharmacia) and eluted with glutathione as per the manufacturer instructions. In some experiments, the protein was further purified by ion exchange chromatography (HiTrap Q, Pharmacia).

### Crystallization and Data Collection

Crystals of the THC-ER $\alpha$  LBD-GRIP1 NR box II peptide complex were prepared by hanging drop vapor diffusion at 19-21°C. Prior to crystallization, the THC-ER $\alpha$  LBD complex was incubated overnight with a four-fold molar excess of the GRIP1 NR box II peptide. Samples (0.5  $\mu$ L) of this solution (5.0 mg/mL protein) were mixed with 3.5  $\mu$ L of reservoir buffer consisting of 16% (w/v) PEG 4000, 53 mM Tris·Cl (pH 8.8) and 50 mM MgCl<sub>2</sub> and suspended over wells containing 800  $\mu$ L of the reservoir buffer. The crystals that formed lie in the spacegroup P2<sub>1</sub> with cell dimensions  $a=54.55$  Å,  $b=82.60$  Å,  $c=59.04$  Å and  $\beta=111.53^\circ$ . Two independent THC-LBD-peptide

complexes form the asymmetric unit. A crystal was transferred to a cryosolvent solution containing 20% (w/v) PEG 4000, 15% (w/v) ethylene glycol, 100 mM Tris·Cl (pH 8.6), 100 mM MgCl<sub>2</sub> and frozen in an N<sub>2</sub> stream in a nylon loop. Diffraction data were measured at -170°C at beamline 5.0.2 at the Advanced Light Source (ALS) using a Quantum 4 CCD camera (Area Detector Systems Corporation) at a wavelength of 1.10 Å. Images were processed with DENZO<sup>35</sup> and the integrated intensities were scaled with SCALEPACK<sup>35</sup> using the default -3σ cutoff.

Crystals of the THC-ERβ LBD complex were obtained by hanging drop vapor diffusion at 21-23°C. Samples (2 μL) of a solution of the complex (4.8 mg/mL) were combined with 2 μL samples of a reservoir solution containing 1.5-1.75 M (NH<sub>4</sub>)<sub>2</sub>SO<sub>4</sub> and 100 mM NaOAc pH 4.8-5.2 and suspended over wells containing 800 μL of reservoir solution. The resulting crystals belong to the space group R3 with cell parameters a=b=99.14 Å and c=193.38 Å (hexagonal setting). The asymmetric unit contains two ERβ LBD monomers which do not interact to form the same dimer seen in the ERα complex. Instead, each of the two LBDs interacts similarly with symmetry-related molecules to form crystallographic trimers. Prior to data collection, a single crystal was transferred to a stabilizing solution (1.8 M (NH<sub>4</sub>)<sub>2</sub>SO<sub>4</sub>, 100 mM NaCl, 100 mM NaOAc pH 4.5, and 10 μM THC). The crystal was then sequentially transferred at 30 minute intervals through a series of solutions consisting of the stabilizing solution supplemented with increasing concentrations of ethylene glycol (1% increments) to a final concentration of 15%. The crystal was then flash frozen in an N<sub>2</sub> stream in a nylon loop. Diffraction data were measured at -170°C at beamline 5.0.2 at the ALS using a Quantum 4 CCD camera at a wavelength of 1.07 Å. Images were processed with DENZO and the integrated intensities were scaled with SCALEPACK using the default -3σ cutoff.

## Structure Determination and Refinement

### *THC-ERα LBD-GRIP1 NR Box II Peptide Complex*

The model of the DES-ER $\alpha$  LBD-GRIP1 NR Box II peptide complex (3ERD) was modified by converting the side chains of certain ligand binding pocket residues (Met 343, Leu 346, Glu 353, Leu 384, Leu 387, Met 388, Leu 391, Arg 394, Phe 404, Met 421, Ile 424, Leu 428, His 524, Leu 525, Met 528, and Leu 540) of both monomers to alanine and by removing all ligands, waters, carboxymethyl groups, and ions. After subjecting this edited model to rigid body refinement in REFMAC<sup>36</sup>, the missing parts of the model were built, and the rest of the model was corrected using MOLOC<sup>37</sup> and two-fold averaged maps generated with DM<sup>36</sup>. All masks for averaging were generated using MAMA<sup>38</sup>, and PHASES<sup>39</sup> and the CCP4 suite<sup>36</sup> were used for the generation of structure factors and the calculation of weights. Initially, positional refinement was performed using REFMAC. At later stages, the model was refined using the simulated annealing, positional and B-factor refinement protocols in CNS<sup>40</sup>. All B-factors were refined isotropically. Anisotropic scaling and a bulk solvent correction were used throughout refinement. The  $R_{\text{free}}$  set contains a random sample of 6.5% of all data. All data between 47 and 1.95 Å (with no  $\sigma$  cutoff) were used. The current model is composed of residues 305 to 459 and 469 to 547 of monomer A, residues 305 to 460 and 472 to 547 of monomer B, residues 687 to 696 of peptide A, residues 686 to 695 of peptide B, two ligand molecules, 167 water molecules, one carboxymethyl group, and one chloride ion. According to PROCHECK<sup>36</sup>, XXX of all residues in the model are in the core regions of the Ramachandran plot, and none are in the disallowed regions.

#### *THC-ER $\beta$ LBD Complex*

The intensities within the ER $\beta$  data set fall off very rapidly as a function of resolution (Wilson B factor  $\sim 90$  Å<sup>2</sup> calculated from 4.5 to 2.85 Å). In order to increase the contribution of the higher resolution terms the data were sharpened with a correction factor of  $-50$  Å<sup>2</sup>. All subsequent manipulations were performed using this sharpened data.

The two LBDs in the asymmetric unit were located by molecular replacement in AMoRe<sup>36</sup> and TFFC<sup>36</sup>. The search model was constructed by overlapping the models of five ER $\alpha$  LBD complexes (PDB Accession Numbers 1A52, 1ERE, 1ERR, 3ERD, and 3ERT) and setting the occupancies of each model to 20% ( $R = 55.3\%$ ,  $CC = 55.9\%$  after placement of both monomers). The model was then rebuilt using MOLOC and two-fold averaged maps generated with DM. MAMA was used for all mask manipulations, and PHASES and the CCP4 suite were used for the generation of structure factors and the calculation of weights. Refinement was performed initially using the positional refinement protocols in REFMAC, and later using the simulated annealing, positional and B-factor refinement protocols in CNS. All B-factors were refined isotropically. Anisotropic scaling, a bulk solvent correction, and tight noncrystallographic symmetry restraints were used throughout refinement. The  $R_{\text{free}}$  set contains a random sample of 5% of all data. All data between 49 and 2.85 Å (with no  $\sigma$  cutoff) were used. The current model is composed of residues 261 to 284, 290 to 408, and 413 to 501 of monomer A, the last residue of the affinity tag and residues 256 to 280, 294 to 410, 413 to 479, and 485 to 497 of monomer B, two ligand molecules, and 9 water molecules. According to PROCHECK, XXX of all residues in the model are in the core regions of the Ramachandran plot, and none are in the disallowed regions.

### Peptide Binding Assay

Samples of the GST-ER $\beta$  LBD fusion protein, in the absence or presence of the various ligands (at saturating concentrations), were mixed with an LXXLL-motif containing peptide (ILRKLLQE), which had been N-terminally labeled with rhodamine (reaction buffer = 10 mM HEPES/Na, 150 mM NaCl, 2 mM MgCl<sub>2</sub>, 1 mM EDTA, and 100  $\mu\text{g}/\text{mL}$  BSA at pH 7.9 and [peptide] = 5 nM). The binding reactions were incubated at ambient temperature with shaking for 1 hour in 96-well plates (Whatman), and the fluorescence polarization was measured on an Analyst reader (Molecular Devices). Receptor concentrations were determined by radioligand

binding<sup>41</sup>.  $K_d$  values were generated from triplicate assays by fitting the data to a simple binding isotherm (Prism, GraphPad Software).

### **Illustrations**

Figures 2A, 2B, 4A, 4C, and 5 were generated using BOBSCRIPT<sup>42</sup> and rendered using Raster3D<sup>43</sup>.

## Figure Legends

### Figure 1 THC Regulates ER AF-2 Activity in a Subtype-selective Manner

- A. Chemical structures of 17 $\beta$ -estradiol (E2), ICI 164,384 (ICI), diethylstilbestrol (DES), 4-hydroxytamoxifen (OHT), and (R,R)-5,11-*cis*-diethyl-5,6,11,12-tetrahydrochrysene-2,8-diol (THC). The side chains of ICI and OHT are highlighted in orange.
- B. E2- and THC-mediated transcriptional response of GAL4-ER LBD chimeras in transiently transfected MDA-MB-231 breast carcinoma cells. Both chimeras activate transcription in the presence of 10 nM E2, but only the ER $\alpha$  chimera activates in the presence of 1  $\mu$ M THC. Values represent the mean  $\pm$  SD for each experimental condition performed in triplicate.

### Figure 2 Overall Structures of the THC-ER LBD Complexes

- A. Two equivalent orthogonal views of the THC-ER $\alpha$  LBD-GRIP1 NR box II peptide and the THC-ER $\beta$  LBD complexes, showing that the two ER LBDs adopt distinct conformations when bound to THC. Both the ER $\alpha$  and ER $\beta$  LBDs are depicted in ribbon representation, and are colored light green and light blue, respectively. In both complexes, helix 12 is colored red, and THC, shown in spacefilling representation, is colored green. In the ER $\alpha$  complex, the coactivator peptide is depicted as a purple ribbon.
- B. Superpositions of the C $\alpha$  trace of the THC-ER $\beta$  LBD complex (cyan) on those of the RAL-ER $\beta$  LBD (orange) and the GEN-ER $\beta$  LBD complexes (yellow). Helix 12 in the RAL and GEN structures is colored red. Least squares superpositions were generated using LSQMAN<sup>44</sup> (THC/RAL: 0.95 Å r.m.s.d. over 196 matched atoms with a 3.8 Å cutoff, THC/GEN: 1.06 Å r.m.s.d. over 218 matched atoms with a 3.8 Å cutoff ).

### Figure 3 Ligands Perturb the Equilibrium Between Two Distinct Conformations of Helix 12

- A. Schematic representation of the effects of different classes of ligands on the described helix 12 conformational equilibrium. Helix 12, colored red, is depicted in two conformations: the "inactive" apo/THC-or GEN-bound conformation and the "active" agonist-bound conformation. The inactive conformation prevents coactivator association, and the active one favors it.
- B. Equilibrium binding of a rhodamine-labeled LXXLL-motif containing peptide to the ER $\beta$  LBD alone or bound to E2, DES, GEN, and THC was analyzed by measuring fluorescence polarization as a function of receptor or ligand-receptor complex concentration. Values represent the mean  $\pm$  SD for each experimental condition performed in triplicate and the data were fit to a simple binding isotherm.

### Figure 4 THC Interactions with the ER $\alpha$ and ER $\beta$ Ligand Binding Pockets

- A.  $2F_o - F_c$  electron density of THC in the ER $\alpha$  complex (green) and in the ER $\beta$  complex (orange). For the ER $\alpha$  complex, the map was calculated to 1.95 Å and contoured at 1.2 $\sigma$ , and for the ER $\beta$  complex, the map was calculated to 2.85 Å and contoured at 1.0 $\sigma$ . Both maps were calculated after omitting the ligand. The ethyl groups of THC are rotated under the tetrahydrochrysene scaffold when bound to ER $\alpha$ , but are rotated outwards when bound to ER $\beta$ .
- B. Schematic diagrams of the interactions between THC and the binding pockets of the two ERs. Only residues or waters that form hydrogen bonds with THC and/or van der Waals contacts with THC (4.2 Å cutoff) are depicted. Hydrogen bonds and van der Waals contacts are represented by cyan lines and gray lines, respectively. Hydrogen bond distances (in Å) are given. Residues that only interact with THC in the ER $\alpha$  complex are green and those that only interact in the ER $\beta$  complex are blue. The A and A' rings and the individual atoms of THC are labeled.
- C. The structures of the two THC-ER complexes were superimposed using LSQMAN (1.13 Å r.m.s.d. over 200 matched C $\alpha$  atoms using a 3.8 Å cutoff). ER $\alpha$  and



ER $\beta$  residues are labeled in light green and light blue, respectively. Side chain atoms are colored by atom type (carbon(ER $\alpha$ )=light green, carbon(ER $\beta$ )=light blue, nitrogen=dark blue, oxygen=red, sulfur=yellow). THC in the ER $\alpha$  complex is colored green and THC in the ER $\beta$  complex is colored orange. Hydrogen bonds are depicted as dashed dark gray bonds. For clarity, water molecules and the side chains of Thr 347 and Leu 349 from ER $\alpha$  and Thr 299 and Leu 301 from ER $\beta$  are not shown.

### **Figure 5 Model of THC-ER $\beta$ LBD in the Agonist-Bound Conformation**

A model of THC-ER $\beta$  LBD complex in the agonist-bound conformation was generated by overlapping the A ring of THC with that of GEN in the GEN-ER $\beta$  complex and optimally positioning the THC scaffold between the side chains of Met 336 and Ile 373. This model and the structure of the THC-ER $\beta$  complexes were superimposed on that of the THC-ER $\alpha$  complex using LSQMAN. For the two crystallographically-determined THC-ER complexes, side chain atoms and THC are colored as in Figure 4C. For the modeled complex, THC is colored red, carbon side chains are colored magenta, and sulfur side chain atoms are colored yellow. Semi-transparent van der Waals surfaces for one of the THC ethyl groups and the side chain of Leu 298 are drawn to illustrate the unfavorable close contacts in the model.

## Acknowledgments

**GRANTS** A. K. S. was supported by a Howard Hughes Medical Institute Predoctoral Fellowship and a UCSF Chancellor's Fellowship. ALS is funded by XXX. We thank M. Butte, N. Ota, and Y. Shibata for assistance with data collection, A. Derman and Y. Li for comments on the manuscript, and H. Deacon for extensive assistance with figures.

## References

1. Curtis Hewitt, S., Couse, J.F. & Korach, K.S. Estrogen receptor knockout mice: What their phenotypes reveal about mechanisms of estrogen action. *Breast Cancer Res.* **2**, 345-352 (2000).
2. Meyers, M.J., Sun, J., Carlson, K.E., Katzenellenbogen, B.S. & Katzenellenbogen, J.A. Estrogen receptor subtype-selective ligands: asymmetric synthesis and biological evaluation of cis- and trans-5,11-dialkyl-5,6,11,12- tetrahydrochrysenes. *J. Med. Chem.* **42**, 2456-2468 (1999).
3. Sun, J. *et al.* Novel ligands that function as selective estrogens or antiestrogens for estrogen receptor-alpha or estrogen receptor-beta. *Endocrinology* **140**, 800-804 (1999).
4. Kraichely, D.M., Sun, J., Katzenellenbogen, J.A. & Katzenellenbogen, B.S. Conformational changes and coactivator recruitment by novel ligands for estrogen receptor-alpha and estrogen receptor-beta: correlations with biological character and distinct differences among SRC coactivator family members. *Endocrinology* **141**, 3534-3545. (2000).
5. Pham, T.A., Hwung, Y.P., Santiso-Mere, D., McDonnell, D.P. & O'Malley, B.W. Ligand-dependent and -independent function of the transactivation regions of the human estrogen receptor in yeast. *Mol. Endocrinol.* **6**, 1043-1050 (1992).
6. Tzukerman, M.T. *et al.* Human estrogen receptor transactivational capacity is determined by both cellular and promoter context and mediated by two functionally distinct intramolecular regions. *Mol. Endocrinol.* **8**, 21-30 (1994).
7. McInerney, E.M., Weis, K.E., Sun, J., Mosselman, S. & Katzenellenbogen, B.S. Transcription activation by the human estrogen receptor subtype beta (ER beta) studied with ER beta and ER alpha receptor chimeras. *Endocrinology* **139**, 4513-4522 (1998).
8. Barkhem, T. *et al.* Differential response of estrogen receptor alpha and estrogen receptor beta to partial estrogen agonists/antagonists. *Mol. Pharmacol.* **54**, 105-112 (1998).

- 9.Kato, S. *et al.* Molecular mechanism of a cross-talk between oestrogen and growth factor signalling pathways. *Genes Cells* **5**, 593-601 (2000).
- 10.Steinmetz, A.C., Renaud, J.P. & Moras, D. Binding of ligands and activation of transcription by nuclear receptors. *Annu. Rev. Biophys. Biomol. Struct.* **30**, 329-359 (2001).
- 11.Glass, C.K. & Rosenfeld, M.G. The coregulator exchange in transcriptional functions of nuclear receptors. *Genes Dev.* **14**, 121-141. (2000).
- 12.Le Douarin, B. *et al.* A possible involvement of TIF1 alpha and TIF1 beta in the epigenetic control of transcription by nuclear receptors. *EMBO J.* **15**, 6701-6715 (1996).
- 13.Heery, D.M., Kalkhoven, E., Hoare, S. & Parker, M.G. A signature motif in transcriptional co-activators mediates binding to nuclear receptors. *Nature* **387**, 733-736 (1997).
- 14.Ding, S.F. *et al.* Nuclear receptor-binding sites of coactivators glucocorticoid receptor interacting protein 1 (GRIP1) and steroid receptor coactivator 1 (SRC-1): Multiple motifs with different binding specificities. *Mol. Endocrinol.* **12**, 302-313 (1998).
- 15.Torchia, J. *et al.* The transcriptional co-activator p/CIP binds CBP and mediates nuclear-receptor function. *Nature* **387**, 677-684 (1997).
- 16.Gampe, R.T., Jr. *et al.* Asymmetry in the PPAR gamma/RXR alpha crystal structure reveals the molecular basis of heterodimerization among nuclear receptors. *Mol. Cell* **5**, 545-555. (2000).
- 17.Darimont, B.D. *et al.* Structure and specificity of nuclear receptor-coactivator interactions. *Genes Dev.* **12**, 3343-3356 (1998).
- 18.Nolte, R.T. *et al.* Ligand binding and co-activator assembly of the peroxisome proliferator-activated receptor gamma. *Nature* **395**, 137-143 (1998).
- 19.Shiau, A.K. *et al.* The structural basis of estrogen receptor/coactivator recognition and the antagonism of this interaction by tamoxifen. *Cell* **95**, 927-937 (1998).
- 20.Bourguet, W. *et al.* Crystal structure of a heterodimeric complex of RAR and RXR ligand-binding domains. *Mol. Cell* **5**, 289-298 (2000).
- 21.Brzozowski, A. *et al.* Molecular basis of agonism and antagonism in the oestrogen receptor. *Nature* **389**, 753-758 (1997).

- 22.Pike, A.C. *et al.* Structure of the ligand-binding domain of oestrogen receptor beta in the presence of a partial agonist and a full antagonist. *EMBO J.* **18**, 4608-4618 (1999).
- 23.Pike, A.C. *et al.* Structural insights into the mode of action of a pure antiestrogen. *Structure* **9**, 145-153 (2001).
- 24.Schultz, J.R. *et al.* Role of LXRs in control of lipogenesis. *Genes Dev.* **14**, 2831-2838 (2000).
- 25.Gangloff, M. *et al.* Crystal structure of a mutant hER alpha ligand-binding domain reveals key structural features for the mechanism of partial agonism. *J. Biol. Chem.* **276**, 15059-15065. (2001).
- 26.Tanenbaum, D.M., Wang, Y., Williams, S.P. & Sigler, P.B. Crystallographic comparison of the estrogen and progesterone receptor's ligand binding domains. *Proc. Natl. Acad. Sci. USA* **95**, 5998-6003 (1998).
- 27.Green, S. *et al.* Human oestrogen receptor cDNA: sequence, expression and homology to v-erb-A. *Nature* **320**, 134-139 (1986).
- 28.Greene, G.L. *et al.* Sequence and expression of human estrogen receptor complementary DNA. *Science* **231**, 1150-1154 (1986).
- 29.Mosselman, S., Polman, J. & Dijkema, R. ER beta: identification and characterization of a novel human estrogen receptor. *FEBS Lett.* **392**, 49-53 (1996).
- 30.Singh, S.M., Gauthier, S. & Labrie, F. Androgen receptor antagonists (antiandrogens): Structure-activity relationships. *Curr. Med. Chem.* **7**, 211-247 (2000).
- 31.Fagart, J. *et al.* Antagonism in the human mineralocorticoid receptor. *EMBO J.* **17**, 3317-3325 (1998).
- 32.Souque, A. *et al.* The mineralocorticoid activity of progesterone derivatives depends on the nature of the C18 substituent. *Endocrinology* **136**, 5651-5658 (1995).
- 33.Greene, G.L., Nolan, C., Engler, J.P. & Jensen, E.V. Monoclonal antibodies to human estrogen receptor. *Proc. Natl. Acad. Sci. USA* **77**, 5115-5119 (1980).
- 34.Witkowska, H.E. *et al.* Characterization of bacterially expressed rat estrogen receptor beta ligand binding domain by mass spectrometry: structural comparison with estrogen receptor alpha. *Steroids* **62**, 621-631 (1997).

- 35.Otwinowski, Z. & Minor, W. Processing of x-ray diffraction data collected in oscillation mode. *Methods Enzymol.* **276**, 307-326 (1997).
- 36.Dodson, E.J., Winn, M. & Ralph, A. Collaborative Computational Project, Number 4: Providing programs for protein crystallography. *Methods Enzymol.* **277**, 620-634 (1997).
- 37.Muller, K. *et al.* MOLOC: A molecular modeling program. *Bull. Soc. Chim. Belg.* **97**, 655-667 (1988).
- 38.Kleywegt, G.J. & Jones, T.A. Software for handling macromolecular envelopes. *Acta Crystallogr. D* **55**, 941-944. (1999).
- 39.Furey, W. & Swaminathan, S. PHASES-95: A program package for processing and analyzing diffraction data from macromolecules. *Methods Enzymol.* **277**, 590-619 (1997).
- 40.Brunger, A.T. *et al.* Crystallography & NMR System: A new software suite for macromolecular structure determination. *Acta Crystallogr. D* **54**, 905-921 (1998).
- 41.Greene, G.L. *et al.* Purification of T47D human progesterone receptor and immunochemical characterization with monoclonal antibodies. *Mol. Endocrinol.* **2**, 714-726 (1988).
- 42.Esnouf, R.M. An extensively modified version of MolScript that includes greatly enhanced coloring capabilities. *J. Mol. Graph. Model.* **15**, 132-134, 112-133 (1997).
- 43.Merritt, E.A. & Bacon, D.J. Raster3D: Photorealistic molecular graphics. *Methods Enzymol.* **277**, 505-524 (1997).
- 44.Kleywegt, G.J. & Jones, T.A. Detecting folding motifs and similarities in protein structures. *Methods Enzymol.* **277**, 525-545 (1997).

**Table 1:** Summary of Crystallographic Statistics

Data Collection	
Complex	THC-ER $\alpha$ LBD-GRIP1 NR      THC-ER $\beta$ LBD
Space group	P2 <sub>1</sub> R3
Resolution	1.95      2.85
Observations	119409      71300
Unique	34533      16522
Completeness (%)	97.9      99.7
R <sub>sym</sub> (%) <sup>a</sup>	6.5      4.7
Average I/ $\sigma$ I	12.3      14.8
Refinement	
Non-hydrogen protein atoms	3830      3409
Water molecules	167      9
Non-hydrogen heterogen atoms	53      48
R <sub>cryst</sub> (%) <sup>b</sup> /R <sub>free</sub> (%)	20.3/24.2      26.5/30.4
Bond r.m.s. deviation (Å)	0.005      0.011
Angle r.m.s. deviation (°)	1.08      1.29
Average B factor (Å <sup>2</sup> )	38.5      40.1

<sup>a</sup>R<sub>sym</sub> =  $\sum |I_h - \langle I_h \rangle| / \sum I_h$ , where  $\langle I_h \rangle$  is the average intensity over symmetry equivalents.

<sup>b</sup>R<sub>cryst</sub> =  $\sum |F_o - F_c| / \sum |F_o|$ , where F<sub>o</sub> and F<sub>c</sub> are observed and calculated amplitudes, respectively.

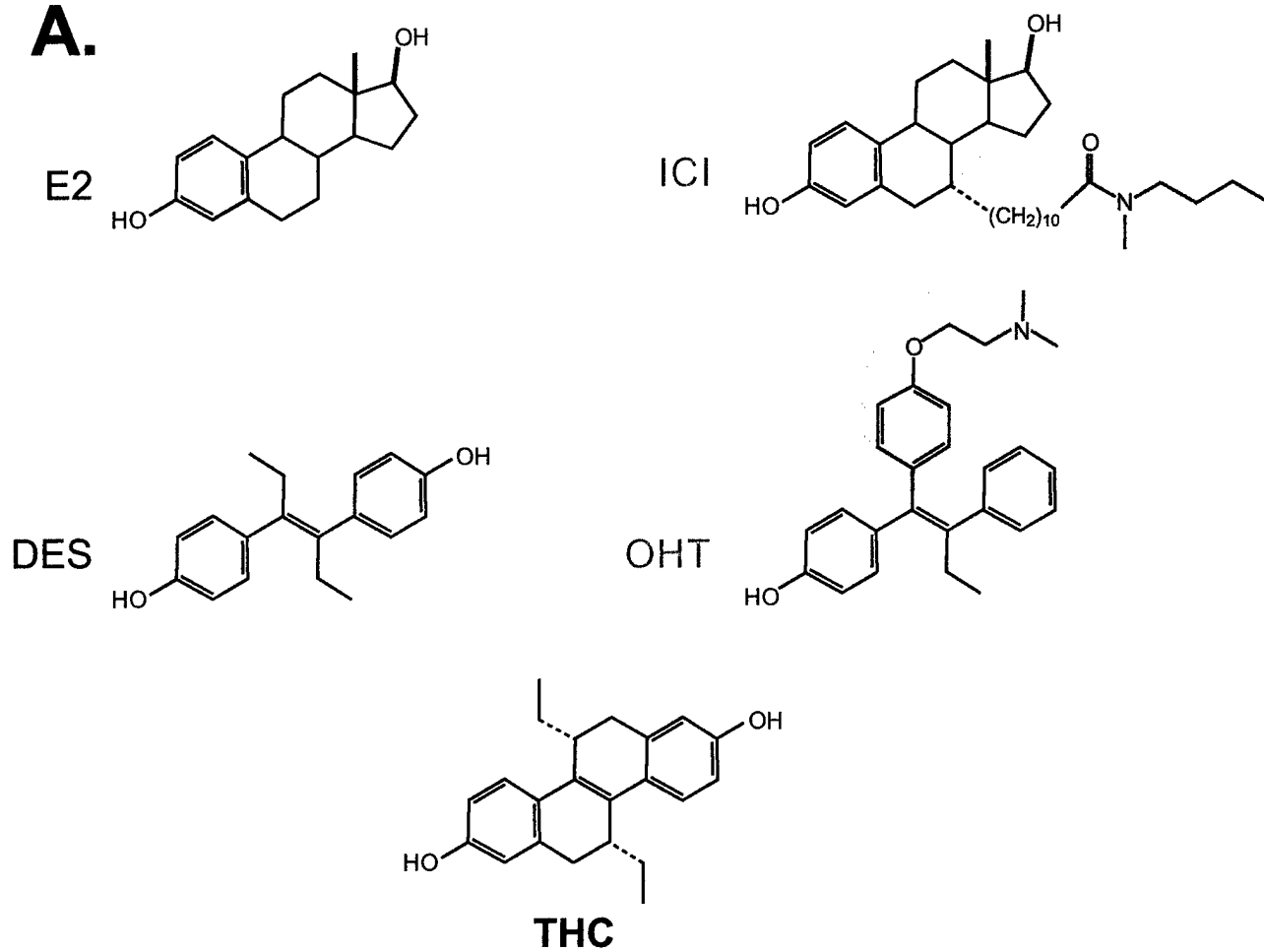
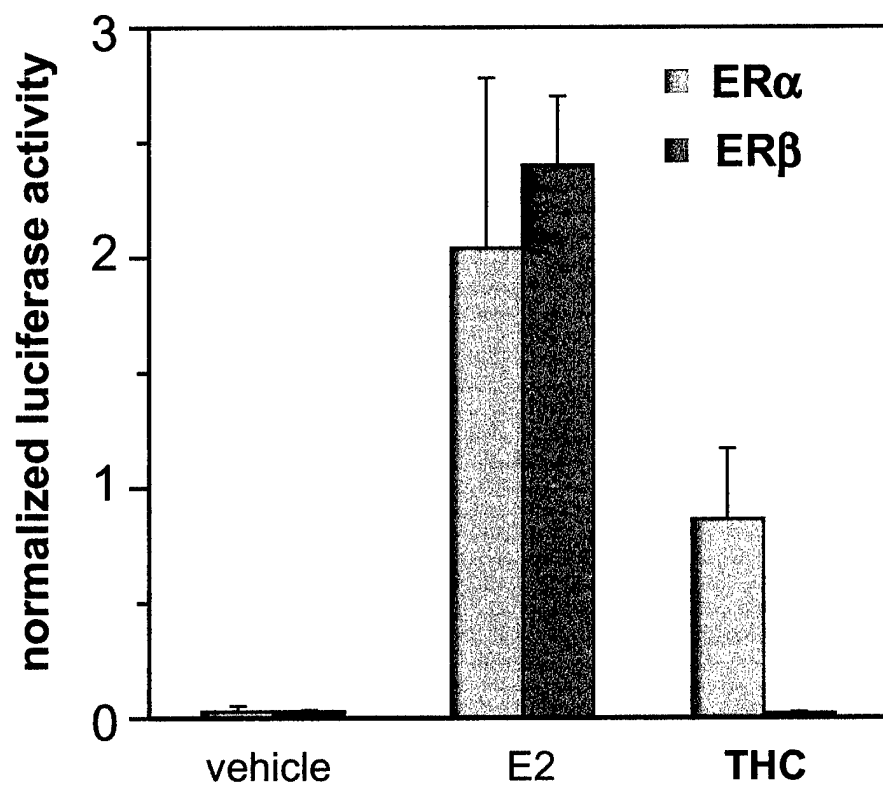
**A.****B.**

Figure 1



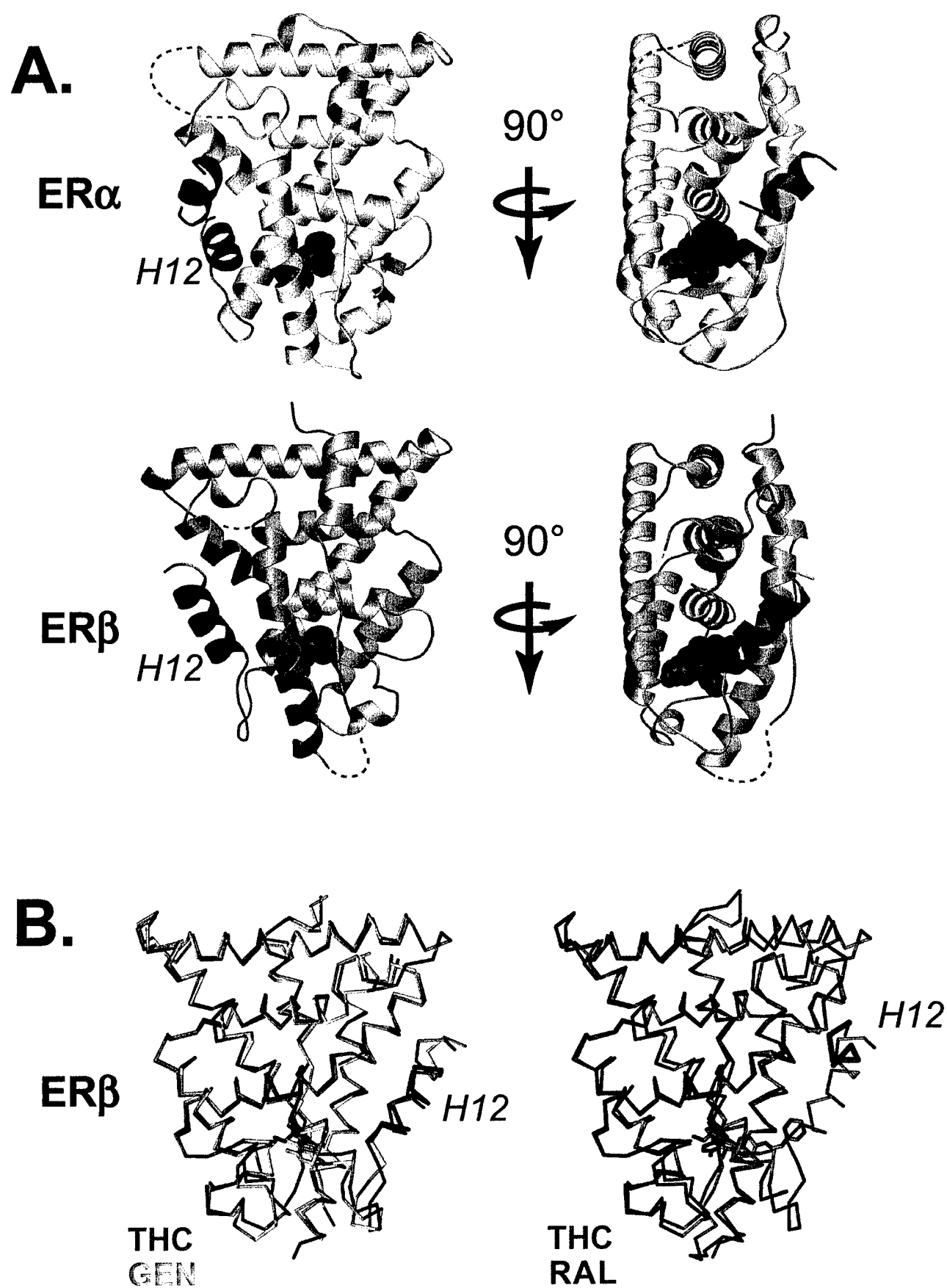


Figure 2

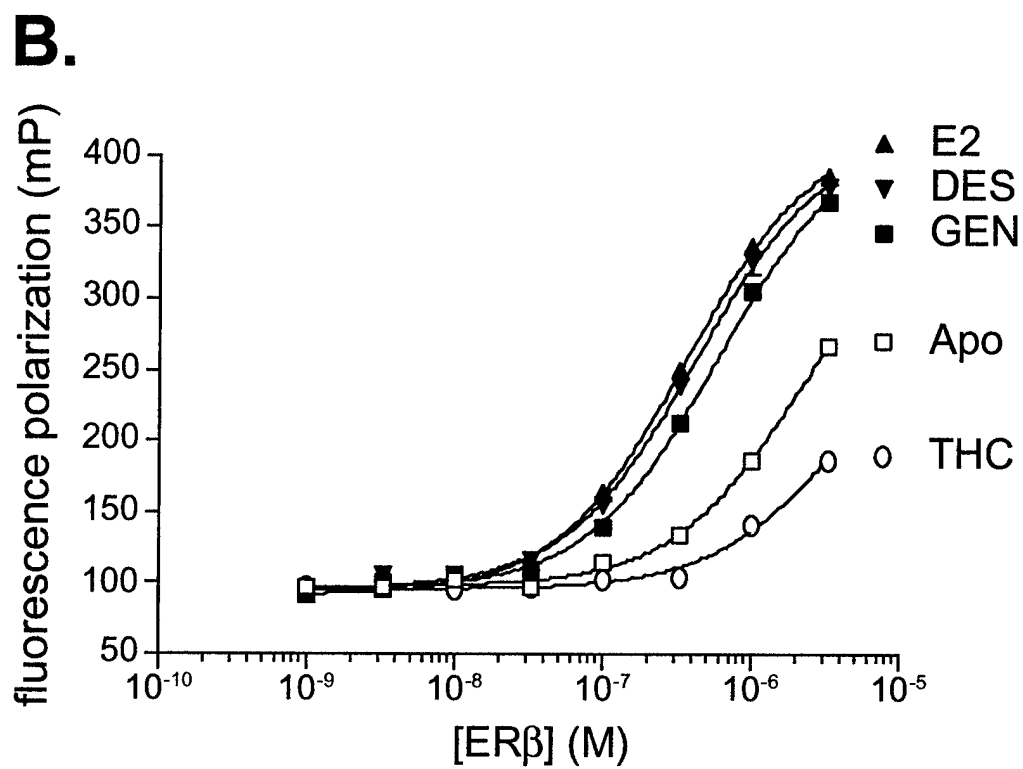
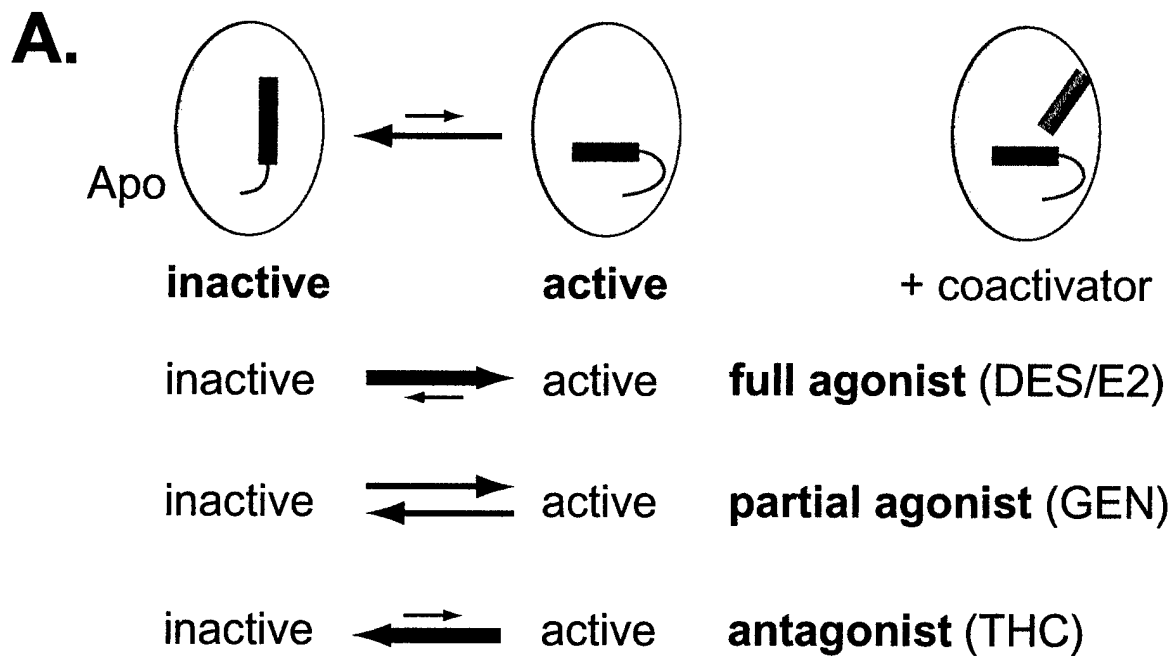
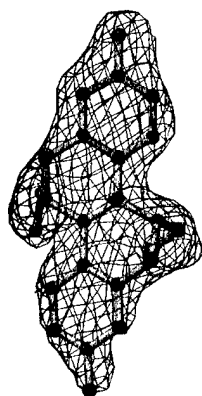
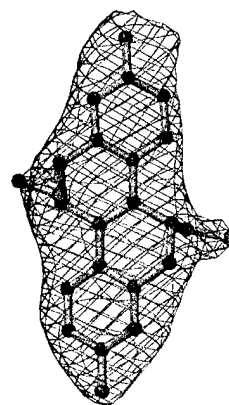


Figure 3

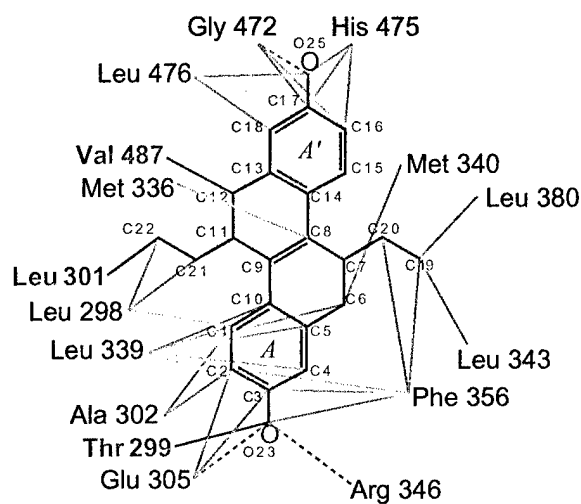
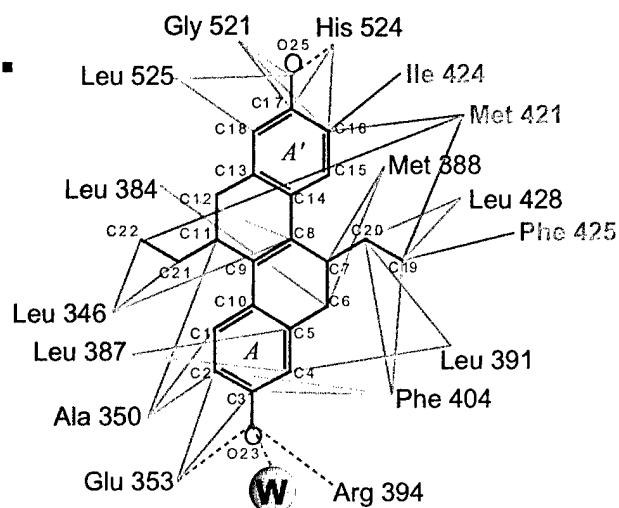
**A.** ER $\alpha$



ER $\beta$



**B.**



**C.**

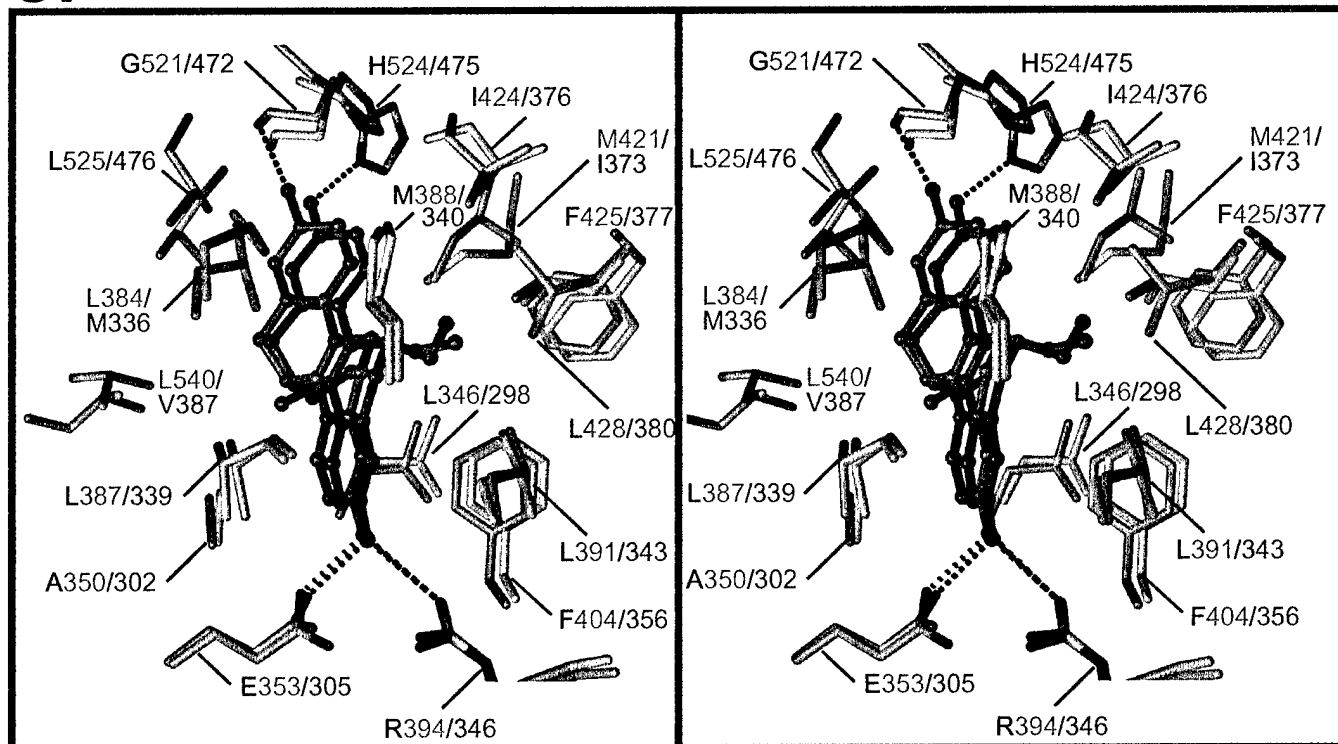


Figure 4

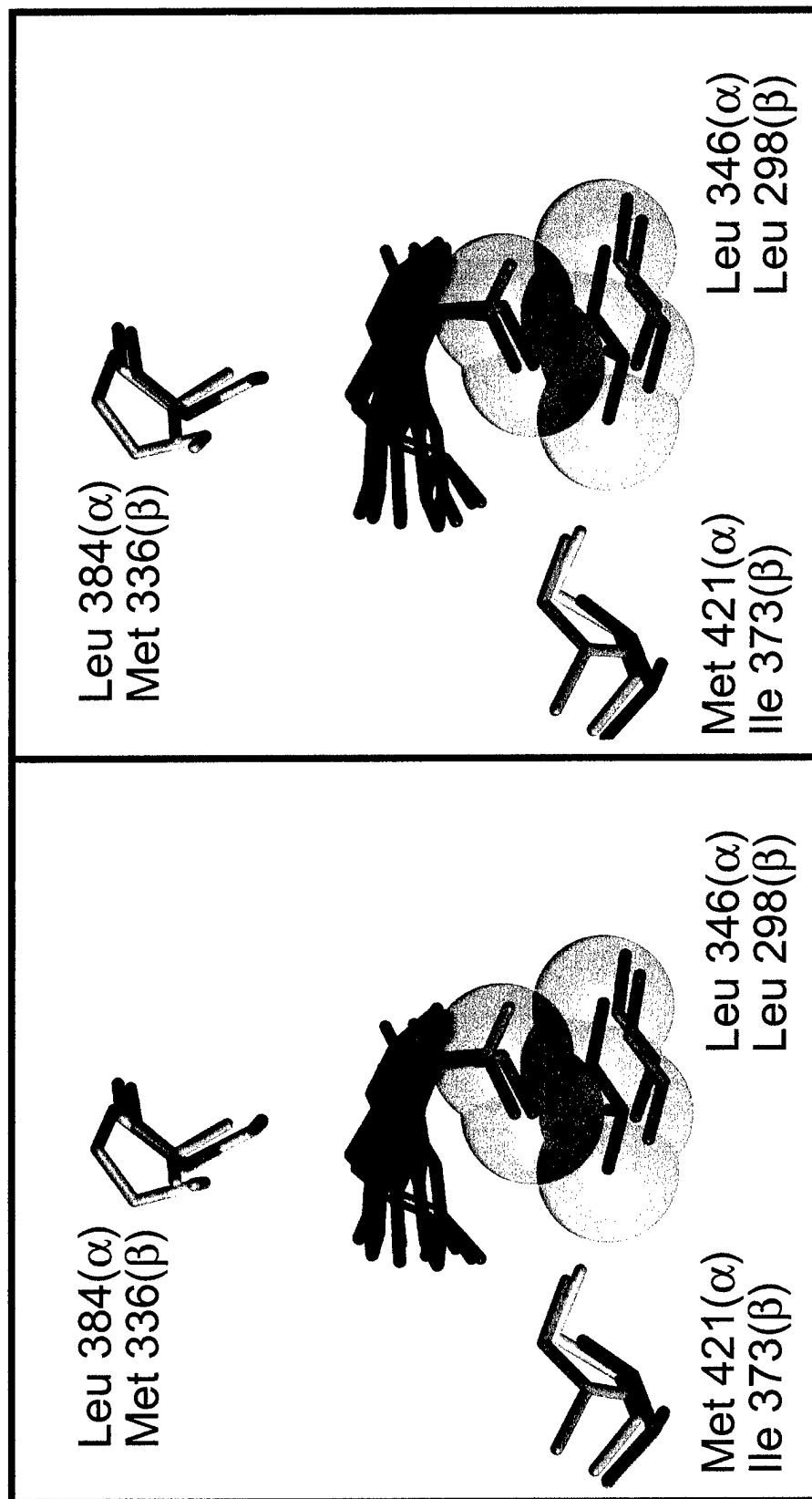


Figure 5

## 01-L

### STRUCTURAL AND MECHANISTIC ASPECTS OF SERM ACTION MEDIATED BY ER $\alpha$ AND ER $\beta$ .

G. L. Greene,<sup>+</sup> A. Shiau,<sup>\*</sup> D. Barstad,<sup>+</sup> P. Kushner,<sup>±</sup> and D. Agard<sup>\*</sup>. <sup>+</sup>Ben May Institute for Cancer Research and Department of Biochemistry and Molecular Biology, University of Chicago, Chicago, Illinois 60637; <sup>\*</sup>Howard Hughes Medical Institute and the Department of Biochemistry & Biophysics, University of California at San Francisco; <sup>±</sup>Metabolic Research Unit, University of California at San Francisco, San Francisco, CA 94143, U.S.A.

Estrogens and estrogen antagonists induce characteristic conformational changes in the estrogen receptor (ER $\alpha$ / $\beta$ ) that influence dimerization, phosphorylation, interaction with general and specific effector molecules, recognition of specific DNA response elements in target genes, and modulation of transcriptional activity. Many of these processes are tissue- and promoter-specific, which can change the balance between the agonistic or antagonistic behavior of a given ligand. Tamoxifen and raloxifene represent a growing class of diverse molecules known as selective estrogen receptor modulators (SERMs), which can be distinguished from pure estrogens by their ability to act either as estrogens (agonist) or as antiestrogens (antagonist) in different tissues, gene contexts and hormone environments. To better understand this selective behavior, the structures of the human ER $\alpha$  ligand binding domain (ER $\alpha$ -LBD) complexed with several estrogen agonists and antagonists were determined. Insight into the molecular basis of estrogen agonism and antagonism has been revealed by the crystal structures of ER $\alpha$  and ER $\beta$  ligand binding domains (LBDs) complexed with several ligands, including estradiol (E2), diethylstilbestrol (DES), raloxifene (RAL), 4-hydroxy-tamoxifen (OHT), and genistein (GEN). For agonists like DES, inclusion of a peptide derived from an essential LXXLL interaction motif (NR box) found in several related p160 nuclear receptor transcriptional co-activators has helped define the AF-2/co-activator interface. Although agonists and antagonists bind at the same site within the core of the LBD, each induces distinct conformations in the transactivation domain (AF-2) of the LBD, especially in the positioning of helix 12, providing structural evidence for multiple mechanisms of selective antagonism in the nuclear receptor family. Interestingly, the OHT/RAL and DES/E2 structures collectively reveal and define a multipurpose docking site on ER $\alpha$  that can accommodate either helix 12 or one of several co-regulators. In addition, a comparison of the two structures reveals that there are at least two distinct mechanisms by which structural features of OHT promote an "autoinhibitory" helix 12 conformation. Helix 12 positioning can be determined both by steric considerations, such as the presence of an extended side chain in the ligand, and by local structural distortions in and around the ligand binding pocket. Thus, one would predict that effective estrogen antagonists do not necessarily require bulky or extended side chains. It is anticipated that the utilization of subtype-specific interactions in ligand design will allow the creation of new compounds that act differently on the two ERs and possess novel therapeutic properties. In addition, with the design and/or natural occurrence of compounds that selectively target ER $\alpha$  or ER $\beta$ , structure information should help reveal the molecular basis for such behavior.

## Correlations Between ER $\alpha$ / $\beta$ Structure and SERM Behavior

Geoffrey L. Greene, PhD

Insight into the molecular basis of estrogen agonism and antagonism has been revealed by the crystal structures of ER $\alpha$  and ER $\beta$  ligand binding domains (LBDs) complexed with several ligands, including estradiol (E2), diethylstilbestrol (DES), raloxifene (RAL), 4-hydroxy-tamoxifen (OHT), and genistein (GEN). For agonists like DES, inclusion of a peptide derived from an essential LXXLL interaction motif (NR box) found in several related p160 nuclear receptor transcriptional coactivators has helped define the AF-2/co-activator interface. Although agonists and antagonists bind at the same site within the core of the LBD, each induces distinct conformations in the transactivation domain (AF-2) of the LBD, especially in the positioning of helix 12, providing structural evidence for multiple mechanisms of selective antagonism in the nuclear receptor family. Interestingly, the OHT/RAL and DES/E2 structures collectively reveal and define a multipurpose docking site on ER $\alpha$  that can accommodate either helix 12 or one of several coregulators. In addition, a comparison of the two structures reveals that there are at least two distinct mechanisms by which structural features of OHT promote an "autoinhibitory" helix 12 conformation. Helix 12 positioning can be determined both by steric considerations, such as the presence of an extended side chain in the ligand, and by local structural distortions in and around the ligand binding pocket. Thus, one would predict that effective estrogen antagonists do not necessarily require bulky or extended side chains.



The crystallographic structures of *cis*-R,R-diethyl-tetrahydrochrysene (R,R-THC) bound to the ligand binding domains of ER $\alpha$  and ER $\beta$  have recently been determined, suggesting mechanisms by which this compound can act as an ER $\alpha$  agonist and as an ER $\beta$  antagonist. Consistent with the prediction that bulky/extended side chains are not essential for antagonist behavior, R,R-THC antagonizes ER $\beta$  in a manner very different to OHT and

### Lessons learned from the structures of ER $\alpha$ and ER $\beta$ bound to SERMs

Greene GL\* (1), Shiau AK (2), Barstad D (1), Katzenellenbogen JA (3) Katzenellenbogen BS (3) and Agard DA (4).

(1) The Ben May Institute for Cancer Research, University of Chicago, Chicago, Illinois 60637 (2) Tularik Inc, South San Francisco, California 94080 (3) Dept. of Chemistry and Dept. of Molecular and Integrative Physiology, University of Illinois, Urbana, Illinois 61801. (4) Howard Hughes Medical Institute and Dept. of Biochemistry & Biophysics, University of California, San Francisco, CA 94143.

Insight into the molecular basis of estrogen agonism and antagonism has been revealed by the crystal structures of ER $\alpha$  and ER $\beta$  ligand binding domains (LBDs) complexed with several ligands, including estradiol (E<sub>2</sub>), diethylstilbestrol (DES), raloxifene (RAL), 4-hydroxy-tamoxifen (OHT), and genistein (GEN). For agonists like DES, inclusion of a peptide derived from an essential LXXLL interaction motif (NR box) found in several related p160 nuclear receptor transcriptional co-activators has helped define the AF-2/co-activator interface. Although agonists and antagonists bind at the same site within the core of the LBD, each induces distinct conformations in the transactivation domain (AF-2) of the LBD, especially in the positioning of helix 12, providing structural evidence for multiple mechanisms of selective antagonism in the nuclear receptor family. Interestingly, the OHT/RAL and DES/ E<sub>2</sub> structures collectively reveal and define a multipurpose docking site on ER $\alpha$  that can accommodate either helix 12 or one of several coregulators. In addition, a comparison of the two structures reveals that there are at least two distinct mechanisms by which structural features of OHT promote an "autoinhibitory" helix 12 conformation. Helix 12 positioning can be determined both by steric considerations, such as the presence of an extended side chain in the ligand, and by local structural distortions in and around the ligand binding pocket. Thus, one would predict that effective estrogen antagonists do not necessarily require bulky or extended side chains.

The crystallographic structures of cis-R, R-diethyl-tetrahydrochrysene (R,R-THC) bound to the ligand binding domains of ER $\alpha$  and ER $\beta$  have recently been determined, suggesting mechanisms by which this compound can act as an ER $\alpha$  agonist and as an ER $\beta$  antagonist. Consistent with the prediction that bulky/extended side chains are not essential for antagonist behavior, R,R-THC antagonizes ER $\beta$  in a manner very different from OHT and RAL, by filling the ligand-binding pocket of ER $\beta$  sub-optimally and acting as a passive antagonist. Interestingly, while the R,R-THC- ER $\beta$  structure is similar to the published GEN- ER $\beta$  structure, the more extensive interactions of genistein with the residues that line the binding pocket of ER $\beta$  may partially shift the helix 12 equilibrium more toward the agonist-bound conformation, consistent with the partial agonism reported for genistein on ER $\beta$ . In contrast, when bound to ER $\alpha$ , R,R-THC is able to induce the agonist-bound conformation of helix 12 by making most of the same contacts as diethylstilbestrol (DES) or estradiol. It is anticipated that the utilization of subtype-specific interactions in ligand design will allow the creation of new compounds that act differently on the two ERs and possess novel therapeutic properties. In addition, with the design and/or natural occurrence of compounds that selectively target ER $\alpha$  or ER $\beta$ , structure information should help reveal the molecular basis for such behavior.

### Molecular Basis of Estrogen Responsiveness

Geoffrey L. Greene. The Ben May Institute for Cancer Research, University of Chicago, Chicago, Illinois 60637

Estrogens and SERMs (selective estrogen receptor modulators) regulate diverse cellular activities via one or both of two known estrogen receptor subtypes ( $ER\alpha$  and  $ER\beta$ ) in hormone responsive tissues and cancers. Liganded ERs can interact with a complex mix of coactivators, corepressors and other signaling molecules that differ in expression and importance from tissue to tissue. In addition, different SERMs may alter the affinity and/or selectivity of one or both ERs for these coregulators, allowing for tissue selective responses. Recently, insight into the molecular basis of estrogen agonism and antagonism has been revealed by the crystal structures of  $ER\alpha$  and  $ER\beta$  ligand binding domains (LBDs) complexed with several ligands, including estradiol (E2), diethylstilbestrol (DES), raloxifene (RAL), 4-hydroxytamoxifen (OHT), and the phytoestrogen genistein (GEN). For agonists like DES, inclusion of a peptide derived from an essential LXXLL interaction motif (NR box) found in several related p160 nuclear receptor transcriptional co-activators has helped define the AF-2/co-activator interface on ER. Although agonists and antagonists bind at the same site within the core of the LBD, each induces distinct conformations in the transactivation domain (AF-2) of the LBD, especially in the positioning of helix 12, providing structural evidence for multiple mechanisms of selective antagonism in the nuclear receptor family. Interestingly, the OHT/RAL and DES/E2 structures collectively reveal and define a multipurpose docking site on  $ER\alpha$  that can accommodate either helix 12 or one of several coregulators. In addition, a comparison of the two structures reveals that there are at least two distinct mechanisms by which structural features of OHT promote an inhibitory conformation of helix 12. Helix 12 positioning is determined both by steric considerations, such as the presence of an extended side chain in the ligand, and by local structural distortions in and around the ligand binding pocket. Thus, one would predict that effective estrogen antagonists do not necessarily require bulky or extended side chains.

The crystallographic structures of a novel synthetic SERM, *cis*-R, R-diethyl-dihydroxy-tetrahydrochrysene (R,R-THC), bound to the ligand binding domains of  $ER\alpha$  and  $ER\beta$  have recently been determined, suggesting mechanisms by which this mixed activity ligand can function as an  $ER\alpha$  agonist and as an  $ER\beta$  antagonist. Consistent with the prediction that bulky/extended side chains are not essential for antagonist behavior, R,R-THC antagonizes  $ER\beta$  in a manner very different from OHT and RAL, by filling the ligand-binding pocket of  $ER\beta$  sub-optimally and acting as a passive antagonist. It is anticipated that the utilization of ER subtype-specific interactions in ligand design will allow the creation of new compounds that act differently on the two ERs and possess novel therapeutic properties. In addition, with the design and/or natural occurrence of compounds that selectively target  $ER\alpha$  or  $ER\beta$ , structure information should help reveal the molecular basis for such behavior. Ultimately, this information must be coupled with information about expression patterns for both ER subtypes as well as essential coregulatory proteins or intersecting signal pathways to predict the behavior of a given SERM in a responsive tissue.



**Structure/function analyses of SERMs complexed with ER $\alpha$  and ER $\beta$ : mechanistic implications**

Geoffrey L. Greene. The Ben May Institute for Cancer Research, University of Chicago, Chicago, Illinois 60637

Estrogens and SERMs (selective estrogen receptor modulators) regulate diverse cellular activities via one or both of two known estrogen receptor subtypes (ER $\alpha$  and ER $\beta$ ) in hormone responsive tissues and cancers. Liganded ERs can interact with a complex mix of coactivators, corepressors and other signaling molecules that differ in expression and importance from tissue to tissue. In addition, different SERMs may alter the affinity and/or selectivity of one or both ERs for these coregulators, allowing for tissue selective responses. Recently, insight into the molecular basis of estrogen agonism and antagonism has been revealed by the crystal structures of ER $\alpha$  and ER $\beta$  ligand binding domains (LBDs) complexed with several ligands, including estradiol (E2), diethylstilbestrol (DES), raloxifene (RAL), 4-hydroxytamoxifen (OHT), and the phytoestrogen genistein (GEN). For agonists like DES, inclusion of a peptide derived from an essential LXXLL interaction motif (NR box) found in several related p160 nuclear receptor transcriptional co-activators has helped define the AF-2/co-activator interface on ER. Although agonists and antagonists bind at the same site within the core of the LBD, each induces distinct conformations in the transactivation domain (AF-2) of the LBD, especially in the positioning of helix 12, providing structural evidence for multiple mechanisms of selective antagonism in the nuclear receptor family. Interestingly, the OHT/RAL and DES/E2 structures collectively reveal and define a multipurpose docking site on ER $\alpha$  that can accommodate either helix 12 or one of several coregulators. In addition, a comparison of the two structures reveals that there are at least two distinct mechanisms by which structural features of OHT promote an inhibitory conformation of helix 12. Helix 12 positioning is determined both by steric considerations, such as the presence of an extended side chain in the ligand, and by local structural distortions in and around the ligand binding pocket. Thus, one would predict that effective estrogen antagonists do not necessarily require bulky or extended side chains.

The crystallographic structures of a novel synthetic SERM, *cis*-R, R-diethyl-dihydroxy-tetrahydrochrysene (R,R-THC), bound to the ligand binding domains of ER $\alpha$  and ER $\beta$  have recently been determined, suggesting mechanisms by which this mixed activity ligand can function as an ER $\alpha$  agonist and as an ER $\beta$  antagonist. Consistent with the prediction that bulky/extended side chains are not essential for antagonist behavior, R,R-THC antagonizes ER $\beta$  in a manner very different from OHT and RAL, by filling the ligand-binding pocket of ER $\beta$  sub-optimally and acting as a passive antagonist. Paradoxically, the R,R-THC-ER $\beta$  structure is very similar to the published GEN-ER $\beta$  structure, which is difficult to reconcile with the opposing behaviors reported for genistein (partial agonist) and R,R-THC (potent antagonist) mediated by ER $\beta$ . However, if it is assumed that the position of H12 is in dynamic equilibrium with the agonist conformation, it seems likely that the extensive interactions of genistein with the residues that line the binding pocket of ER $\beta$  may partially shift the H12 equilibrium more toward the agonist conformation, consistent with the observed agonism of genistein on ER $\beta$ . R,R-THC is not able to make the same stabilizing contacts in the pocket of the ER $\beta$  LBD, thereby favoring the antagonist conformation of H12. In contrast, when bound to ER $\alpha$  LBD, R,R-THC is able to stabilize the agonist conformation of H12 by making most of the same contacts as diethylstilbestrol (DES) or estradiol. It is anticipated that the utilization of ER subtype-specific interactions in ligand design will allow the creation of new compounds that act differently on the two ERs and possess novel therapeutic properties. In addition, with the design and/or natural occurrence of compounds that selectively target ER $\alpha$  or ER $\beta$ , structure information should help reveal the molecular basis for such behavior. Ultimately, this information must be coupled with information about expression patterns for both ER subtypes as well as essential coregulatory proteins or intersecting signal pathways to predict the behavior of a given SERM in a responsive tissue.